

**UNIVERSITY OF SÃO PAULO  
CENTER FOR NUCLEAR ENERGY IN AGRICULTURE**

**THALITA CAMPOS OLIVEIRA**

**Variability of soil hydraulic properties and its impact on  
agro-hydrological model predictions**

**Piracicaba  
2019**



**THALITA CAMPOS OLIVEIRA**

**Variability of soil hydraulic properties and its impact on agro-hydrological  
model predictions**

**Revised version according to Resolution CoPGr 6018/2011**

**Thesis presented to obtain the degree of Doctor of  
Science at the Center for Nuclear Energy in  
Agriculture of the University of São Paulo**

**Concentration Area: Nuclear Energy in  
Agriculture and Environment**

**Supervisor: Prof. Dr. Quirijn de Jong van Lier**

**Piracicaba**

**2019**

AUTORIZO A DIVULGAÇÃO TOTAL OU PARCIAL DESTE TRABALHO, POR QUALQUER MEIO CONVENCIONAL OU ELETRÔNICO, PARA FINS DE ESTUDO E PESQUISA, DESDE QUE CITADA A FONTE.

Dados Internacionais de Catalogação na Publicação (CIP)

**Seção Técnica de Biblioteca - CENA/USP**

Oliveira, Thalita Campos

Variabilidade das propriedades hidráulicas do solo e seu impacto nas previsões de um modelo agro-hidrológico / Variability of soil hydraulic properties and its impact on agro-hydrological model predictions / Thalita Campos Oliveira; orientador Quirijn de Jong van Lier. - - Versão revisada de acordo com a Resolução CoPGr 6018 de 2011. - - Piracicaba, 2019.

90 p. : il.

Tese (Doutorado – Programa de Pós-Graduação em Ciências. Área de Concentração: Energia Nuclear na Agricultura e no Ambiente) – Centro de Energia Nuclear na Agricultura da Universidade de São Paulo.

1. Água do solo 2. Análise estocástica 3. Balanço de energia 4. Balanço hídrico 5. Manejo do solo 6. Sistema solo-planta-atmosfera I. Título

CDU 631.46 : 626.8

**Elaborada por:**

Marília Ribeiro Garcia Henyei

CRB-8/3631

Resolução CFB Nº 184 de 29 de setembro de 2017

To all women who face the challenge of motherhood and science

Dedicated to  
The light of my life, who showed me pure love and embraced me with kindness  
To my daughter, Laís



## ACKNOWLEDGMENTS

To Professor Quirijn de Jong van Lier for the opportunity to be part of his team; it has been a long but pleasant journey. Thank you for the support and encouragement along these years. Your commitment to science is admirable and has been contagious me.

To my colleagues from FISOL, especially to Victor Meriguetti Pinto, Ali Mehmandoost Kotlar and Leonardo Inforsato, and also to those who already had left the group, especially to André Herman Bezerra, for the scientific (and non-scientific!) discussions we have had along these years. It was a pleasure to share so many moments with you all.

To Professor Jos van Dam for the opportunity to be part of the Soil Physics and Land Management Group at the Wageningen University in The Netherlands as a guest researcher. To Jan Wesseling for his kindness and remarkable scientific contributions to this PhD thesis. Without his patience and dedication, this thesis would likely be incomplete.

To my beloved husband, who has always encouraged me to start this thesis even knowing that it would not be easy living apart for many years. Thank you for your support, comprehension and patience. To my mother who spared no efforts travelling many weekends to help me looking after my daughter. Without your kindness, and above all, love, this study would still possibly be unfinished.

To FAPESP (São Paulo Research Foundation) for funding most of this PhD thesis (grant # 2015/04430-5) and for sponsoring my research internship abroad ((grant # 2017/211109-1). To CAPES (Coordination for the Improvement of Higher Education Personnel - Brazil) for funding part of this PhD thesis – Financing Code 001.



“If you can meet success and failure and treat them both as impostors, then you are a  
balanced man”

Rudyard Kipling



## ABSTRACT

OLIVEIRA, T. C. **Variability of soil hydraulic properties and its impact on agro-hydrological model predictions.** 2019. 90 p. Tese (Doutorado) – Centro de Energia Nuclear na Agricultura, Universidade de São Paulo, Piracicaba, 2019.

Agro-hydrological models have been widely used to predict and simulate soil water balance components and crop yield with reliable results. These models provide detailed water and energy balances and enables simulating scenarios with distinct land management strategies, environmental and climate conditions. However, they require many input parameters, especially those related to soil water retention and hydraulic conductivity functions. These input parameters are prone to variation due to the determination methods, related errors and uncertainties, and soil variability. In this thesis we aimed to (1) analyze the suitability of inverse modelling as an alternative to traditional methods to estimate soil hydraulic properties using water content data obtained with Frequency Domain Reflectometry (FDR) sensors in a field experiment; (2) analyze the influence of the Mualem-van Genuchten parameters (M-VG) uncertainty on water balance components and crop yield predicted by the SWAP model for a soil under maize under rainfed conditions by uncertainty analysis using two sampling methods. One method used Monte Carlo Random Sampling from normal distribution based on standard errors of the hydraulic parameters obtained from inverse modelling (MCRS), and the other used Monte Carlo Latin Hypercube Sampling (MCLHS). Our results from the inverse modelling showed that  $n$  and  $K_s$  from both horizons, and  $\theta_r$  from the Bt horizon, were estimated with low accuracy. Low values of field water contents in the A horizon led to a lower estimate of  $\theta_r$  compared to the laboratory method. In the Bt horizon, the small observed range of field water contents contributed to an unreliable estimation of parameters  $\theta_r$  and  $n$ . The MCRS and MCLHS sampling methods provided distinct ranges and probability density distributions shape for  $n$ -parameter, and simulates runoff ( $R_{off}$ ), soil evaporation ( $E_{soil}$ ) and bottom flux ( $q_{bot}$ ). The M-VG parameters from MCRS may enhanced the uncertainty of simulated results, whereas MCLHS provided more reliable M-VG parameters combinations, and therefore, simulated results. The uncertainty analysis may provide useful information about the uncertainties of model SWAP predictions and should be preferred over a mere deterministic approach, which often provided results diverging those obtained from probabilistic methods. Moreover, the uncertainty analysis is a key tool for more reliable interpretation of the water balance and crop yield in agro hydrological systems and should be considered in agro-modelling studies.

Keywords: Soil hydraulic properties. Inverse modelling. Stochastic realization. Uncertainty analysis. SWAP model.



## RESUMO

OLIVEIRA, T. C. **Variabilidade das propriedades hidráulicas do solo e seu impacto nas previsões de um modelo agro-hidrológico.** 2019. 90 p. Tese (Doutorado) – Centro de Energia Nuclear na Agricultura, Universidade de São Paulo, Piracicaba, 2019.

Modelos agro-hidrológicos têm sido amplamente utilizados para prever e simular os componentes do balanço hídrico e o rendimento de culturas gerando resultados confiáveis. Esses modelos fornecem balanços hídrico e de energia detalhados, além de permitir a simulação de cenários adotando diferentes estratégias de manejo do solo e em diversas condições ambientais e climáticas. No entanto, eles exigem um grande número de parâmetros de entrada, especialmente aqueles relacionados às funções de retenção de água e de condutividade hidráulica do solo. Por sua vez, esses parâmetros são sujeitos a variações provenientes dos métodos de determinação, dos erros e incertezas relacionados a eles, e da variabilidade do solo. Nessa tese objetivou-se (1) analisar a aptidão da modelagem inversa como uma alternativa aos métodos tradicionais para estimar as propriedades hidráulicas do solo utilizando dados de conteúdo de água obtidos por sensores de Reflectometria no Domínio da Frequência (FDR) em um experimento de campo; (2) analisar a influência da incerteza dos parâmetros de Mualem-van Genuchten (M-VG) nos componentes do balanço hídrico e no rendimento de culturas previstos pelo modelo de SWAP para a cultura do milho sem irrigação por meio de análise de incerteza utilizando dois métodos de amostragem. Um método utilizou amostragem aleatória de Monte Carlo baseado nos erros padrão dos parâmetros de M-VG obtidos pela modelagem inversa (MCRS) e a outra utilizou o método de Monte Carlo de amostragem por Hipercubo Latino (MCLHS). Os resultados da modelagem inversa mostraram que os parâmetros  $n$ ,  $K_s$  e  $\theta_r$  do horizonte Bt, foram estimados com baixa precisão. Os baixos valores de conteúdo de água do solo no horizonte A resultaram em valores menores de  $\theta_r$  em comparação com o método de laboratório. No horizonte Bt, a estreita amplitude do conteúdo de água contribuiu para uma estimativa pouco confiável dos parâmetros  $\theta_r$  e  $n$ . Os dois métodos de amostragem resultaram em amplitudes e formatos de funções de densidade de probabilidade distintas para o  $n$ , e escoamento superficial, evaporação do solo e drenagem profunda simulados. O conjunto de parâmetros hidráulicos de M-VG gerados pelo MCRS podem ter aumentado a incerteza dos resultados simulados, enquanto o MCLHS gerou combinações de parâmetros mais prováveis e resultados simulados mais confiáveis. A análise de incerteza pode fornecer informações importantes sobre as incertezas nas previsões do modelo SWAP e deve ser preferida em detrimento à uma abordagem determinística, que geralmente fornece resultados divergentes dos gerados pelo método probabilístico. Além disso, a análise de incerteza é uma ferramenta-chave para a interpretação mais confiável do balanço de água no solo e do rendimento de culturas e deve ser adotado nos estudos de modelagem agro-hidrológica.

Palavras-chave: Propriedades hidráulicas do solo. Modelagem inversa. Realização estocástica. Análise de incerteza. Modelo SWAP.

## LIST OF FIGURES

- Figure 2.1 Schematic representation of the area with the 9 studied sites. Each site contains FDR sensors at its center (cross) for water content monitoring ( $\theta_f$ ), and four sampling locations in the corners for water retention characterization (dots) ( $n = 4$ ). Site #2 (in gray) was not used in this study.
- Figure 2.2 Main daily rainfall, solar radiation and air temperature as observed at the University of São Paulo weather station in Piracicaba/Brazil during the period July - December 2016.
- Figure 2.3 Mean daily water contents from all sites of the experiment ( $\theta_f$ ) ( $n = 9$ ) using FDR sensors (line), and daily rainfall. The colored area represents the minimum and maximum water contents.
- Figure 2.4 One-dimensional soil profile discretization with 40 nodes used in HYDRUS 1-D, showing soil horizons (A: red and B: blue) and sensor positions (squares).
- Figure 2.5 Soil water retention curves obtained by the laboratory method (LM) (points with standard deviation) and fitted by Mualem-van Genuchten model for each site of the experiment ( $n = 9$ ). Bold lines represents the mean curve for each horizon ( $n = 9$ ), thin lines represent the mean of four replicates per site ( $n = 4$ ).
- Figure 2.6 Measured (dots) and simulated (lines) water contents performed with the Mualem-van Genuchten parameters obtained using the laboratory method (LM) and inverse modelling (IM) over time for high and low NSE obtained by the inverse modelling (Site #4 and Site #9, respectively).
- Figure 2.7 Measured and simulated water contents for Site #4 and Site #9 (high and low NSE, respectively, obtained from the inverse modelling) performed with the Mualem-van Genuchten parameters obtained using (a) inverse modelling (IM) and (b) the laboratory method (LM).
- Figure 2.8 Measured water contents ( $\theta_f$ ) and estimated matric potential ( $h_{est}$ ) using the Mualem-van Genuchten parameters obtained by IM during the calibration period for Site #10.

- Figure 2.9 Soil water retention curves derived from laboratory method (LM) and inverse modelling (IM) fitted by Mualem-van Genuchten model for A and Bt horizons for each site of the experiment ( $n = 9$ ). Bold lines represents the mean curve for each horizon ( $n = 9$ ), thin lines represent the mean of four replicates per site ( $n = 4$ ).
- Figure 2.10 Mean Mualem-van Genuchten parameters obtained from laboratory method (LM) and inverse modelling (IM) for A and Bt horizons for all sites of the experiment ( $n = 9$ ). Each Mualem-van Genuchten parameter of LM represents the mean of four replicates ( $n = 4$ ).
- Figure 2.11 Empirical cumulative distribution function of water contents from field measurement ( $\theta_f$ ) for A and Bt horizons for all sites of the experiment ( $n = 9$ ). The dashed line represents water content ( $\theta$ ) at 15000 cm of suction for A and Bt horizons (lines are overlapped).
- Figure 2.12 Mean actual surface ( $q_{sur}$ ) (a) and bottom ( $q_{bot}$ ) (b) flux from all sites of the experiment ( $n = 9$ ) simulated by HYDRUS 1-D using Mualem-van Genuchten parameters obtained from laboratory method (LM) and inverse modelling (IM), and daily rainfall.
- Figure 3.1 Schematic representation of the area with the 9 studied sites. Each site contains FDR sensors at its center (cross) for water content monitoring ( $\theta_f$ ), and four sampling locations in the corners for water retention characterization (dots) ( $n = 4$ ). Site #2 (in gray) was not used in this study.
- Figure 3.2 Main annual rainfall, daily solar radiation and air temperature as observed at the University of São Paulo weather station in Piracicaba/Brazil during the period 1987 – 2017.
- Figure 3.3 Probability density distributions of the Mualem-van Genuchten parameters obtained from Monte Carlo Random Sampling (MCRS) ( $n = 1256$ ) and Monte Carlo Latin Hypercube Sampling (MCLHS) ( $n = 1000$ ). Dashed lines refers to the mean values for MCRS and MCLHS. Mean lines of  $\theta_s$  from Bt horizon are overlapped.
- Figure 3.4 Quantile–quantile plots depicting heavy tails from  $n$  and  $K_s$  probability distributions functions of the Bt horizon based on Monte Carlo Random Sampling (MCRS).

- Figure 3.5 Water retention curves using maximum and minimum values of the Mualem-van Genuchten parameters for Monte Carlo Random Sampling (MCRS) and Monte Carlo Latin Hypercube Sampling (MCLHS) for A and Bt horizons. Thick lines represents the curves using the mean values.
- Figure 3.6 Probability density function of the SWAP results, actual crop yield ( $Y$ ), accumulated season runoff ( $R_{off}$ ), accumulated season plant transpiration ( $T$ ), accumulated season soil evaporation ( $E_{soil}$ ), and accumulated season bottom flux ( $q_{bot}$ ) obtained using Monte Carlo Random Sampling (MCRS) ( $n = 1256$ ) and Monte Carlo Latin Hypercube Sampling (MCLHS) ( $n = 1000$ ). Dashed lines refers to the mean values for each sampling method and the black line refers to deterministic simulation ( $n = 9$ ).
- Figure 3.7 (a) Measured and simulated water contents with the lower limit (0.05 percentile) and upper limit (0.95 percentile) performed by the SWAP model for Monte Carlo Random Sampling (MCRS) ( $n = 1256$ ) and Monte Carlo Latin Hypercube Sampling (MCLHS) ( $n = 1000$ ) for A and Bt horizons. (b) Mean  $\theta_f$  from all sites of the area ( $n = 9$ ) and  $\theta_{50\%}$  for MCRS and MCLHS for A and Bt horizons.



## LIST OF TABLES

- Table 2.1 Particle size distribution and particle density ( $\rho_p$ ), bulk density ( $\rho_b$ ), total porosity (TP, calculated from densities), textural class, and type of structure for A and Bt horizons (mean values with standard deviations between brackets).
- Table 2.2 Statistical model evaluation performance rating for coefficient of determination, ( $r^2$ -eq. 2.4), and Nash-Sutcliffe efficiency (NSE- eq. 2.6) (Moriassi et al., 2015).
- Table 2.3 Mualem-van Genuchten fitting parameters and their descriptive statistics for the laboratory method (LM) and inverse modelling (IM) (standard deviation between brackets).
- Table 2.4 Estimated M-VG parameters (eq. 2.1, 2.2 and 2.3) with standard error and model evaluation coefficients  $r^2$  and RMSE (95% confidence interval between brackets), and NSE for simulated water contents ( $\theta_{sim}$ ) using hydraulic parameters provided by laboratory method (LM) and inverse modelling (IM).
- Table 2.5 Correlation coefficients between Mualem-van Genuchten parameters per horizon and between horizons. Red and blue colors represent the correlation between parameters for A and Bt horizons, respectively; black colors between Mualem-van Genuchten parameters from different horizons. Parameters without correlation are not shown. Correlations  $>0.6$  are indicated by bold numbers.
- Table 3.1 Mualem-van Genuchten parameters (eq. 3.1 and eq. 3.2) and respective standard errors for A and Bt horizons obtained from inverse modelling associated with model evaluation coefficients  $r^2$  and RMSE (95% confidence interval) for all sites of the area (n = 9).
- Table 3.2 Scenario specifications used to perform the SWAP simulations for maize.
- Table 3.3 Statistical characteristics of the Mualem-van Genuchten parameters for Random Sampling (MCRS) (n = 1256) and Monte Carlo Latin Hypercube Sampling (MCLHS) (n = 1000) for A and Bt horizons

Table 3.4 Statistical characteristics of water balance components and crop yield for Monte Carlo Random Sampling (MCRS) and Monte Carlo Latin Hypercube Sampling (MCLHS). Values for runoff, plant transpiration, soil evaporation and bottom flux are cumulative.

Table 3.5 Mean of the ten lower ( $L_{w10}$ ) and upper ( $U_{p10}$ ) Mualem-van Genuchten parameters for Monte Carlo Random Sampling (MCRS) and Monte Carlo Latin Hypercube Sampling (MCLHS) for A and Bt horizons.

## LIST OF SYMBOLS

<b>Symbol</b>	<b>Description (unity)</b>
$\theta$	Volumetric soil water content ( $\text{cm}^3 \text{cm}^{-3}$ )
$\theta_i$	Initial soil water content ( $\text{cm}^3 \text{cm}^{-3}$ )
$\theta_f$	Volumetric soil water content measured in the field ( $\text{cm}^3 \text{cm}^{-3}$ )
$\theta_r$	Residual volumetric soil water content ( $\text{cm}^3 \text{cm}^{-3}$ )
$\theta_s$	Saturated volumetric soil water content ( $\text{cm}^3 \text{cm}^{-3}$ )
$\theta_{50\%}$	50% percentile of simulated water contents ( $\text{cm}^3 \text{cm}^{-3}$ )
$\alpha$	Shape parameter of the soil water retention function ( $\text{cm}^{-1}$ )
$\lambda$	Shape parameter of the soil unsaturated hydraulic conductivity function (-)
$\Theta$	Effective saturation (-)
$a_H$	Interception coefficient of Von Hoyningen-Hune and Braden (-)
$E_{soil}$	Accumulated season soil evaporation (mm)
$h$	Matric potential (cm)
$K$	Unsaturated soil hydraulic conductivity ( $\text{cm d}^{-1}$ )
$K_c$	Crop coefficient (-)
$K_{dif}$	Light extinction coefficient for diffuse visible light (-)
$K_{dir}$	Light extinction coefficient for direct visible light (-)
$K_s$	Saturated soil hydraulic conductivity ( $\text{cm d}^{-1}$ )
$LAI_0$	Leaf area index at the beginning of simulation ( $\text{m}^2 \text{m}^{-2}$ )
$Lw10$	Mean of the ten lower Mualem-van Genuchten parameters
$h_{est}$	Estimated matric potential (cm)
$h_1$	Pressure head above which root water uptake is zero due oxygen deficit (cm)
$h_2$	Pressure head below which root water uptake is optimum (cm)
$h_{3H}$	Pressure head below which root water uptake is reduced due water deficit (high potential transpiration) (cm)
$h_{3L}$	Pressure head below which root water uptake is reduced due water deficit (low potential transpiration) (cm)
$h_4$	Pressure head below which root water uptake is zero due water deficit (cm)

<i>MCRS</i>	Monte Carlo Random Sampling
<i>MCRS</i>	Monte Carlo Latin Hypercube Sampling
<i>n</i>	Shape parameter of the soil water retention function (-)
<i>N</i>	Number of samples
<i>NSE</i>	Nash-Sutcliffe efficiency parameter
<i>q<sub>b</sub></i>	Simulated actual bottom flux (cm d <sup>-1</sup> )
<i>q<sub>bot</sub></i>	Accumulated season bottom flux (mm)
<i>q<sub>sur</sub></i>	Simulated actual surface flux (cm d <sup>-1</sup> )
<i>r<sup>2</sup></i>	Coefficient of determination
<i>R<sub>d</sub></i>	Rooting depth (m)
<i>R<sub>dc</sub></i>	Maximum rooting depth crop (m)
<i>R<sub>di</sub></i>	Initial rooting depth (cm)
<i>R<sub>ri</sub></i>	Maximum daily increase in rooting depth (cm d <sup>-1</sup> )
<i>R<sub>off</sub></i>	Accumulated season runoff (mm)
<i>S</i>	Root water uptake (cm <sup>3</sup> cm <sup>-3</sup> d <sup>-1</sup> )
<i>T</i>	Time (d)
<i>T<sub>a</sub></i>	Actual plant transpiration rate (cm d <sup>-1</sup> )
<i>T</i>	Accumulated season plant transpiration (mm)
<i>Up10</i>	Mean of the ten upper Mualem-van Genuchten parameters
<i>Y</i>	Actual crop yield (kg ha <sup>-1</sup> )
<i>z</i>	Vertical coordinate (m)

## CONTENTS

1	INTRODUCTION.....	23
2	DETERMINING HYDRAULIC PROPERTIES OF A TROPICAL SOIL BY INVERSE MODELLING OF FIELD WATER CONTENTS .....	27
2.1	Introduction	27
2.2	Material and Methods	29
2.2.1	Site description .....	29
2.2.2	Soil hydraulic parametrization.....	31
2.2.3	Model performance evaluation .....	34
2.3	Results and Discussion	35
2.3.1	Soil hydraulic parametrization.....	35
2.3.2	Model performance.....	44
2.3.3	Actual surface ( $q_{sur}$ ) and bottom ( $q_{bot}$ ) flux simulation .....	47
2.4	Conclusions	49
	References	49
3	HYDRAULIC PROPERTIES SAMPLING STRATEGIES AFFECT THE UNCERTAINTY OF VADOSE ZONE HYDROLOGICAL MODEL PREDICTIONS.....	54
3.1	Introduction	54
3.2	Material and Methods	57
3.2.1	Soil hydraulic properties.....	57
3.2.2	Hydrological modelling.....	59
3.2.3	Simulation scenario .....	60
3.2.4	Uncertainty analysis.....	61
3.2.5	Modelling validation	63
3.3	Results and Discussion	63
3.3.1	Hydraulic parameters uncertainty.....	63
3.3.2	Uncertainty of modelling results .....	67
3.3.3	Simulated water contents .....	71
3.4	Conclusions	73
	References	73
4	CONCLUDING REMARKS .....	79
	APPENDIX	79



## 1 INTRODUCTION

Prediction of water movement in soils is one of the most studied subjects in soil physics. The importance of this subject is attached to hydrological cycle and agricultural systems, where processes related to availability of water to plants, transport of solutes in the soil, irrigation and drainage management, soil and water conservation, plant transpiration, crop yield, oxygen and drought stresses, among others, are mostly driven by soil water dynamics. Moreover, this importance extend far beyond hydrology and agriculture, as it has a fundamental role in providing ecosystem services to human well-being (VEREECKEN et al., 2016).

In this context, many hydrological models have been developed aiming to understand the related process and provide reliable information which may be used for supporting water resources management strategies and crop yield optimization in agricultural operations (e.g., CERES-maize, JONES; KINIRY, 1986; MACROS; PENNING DE VRIES et al., 1989; WAVE; VAN-CLOOSTER et al., 1996; SWAP; KROES et al., 1998; HYDRUS 1-D, ŠIMŮNEK et al., 1998; SWAT; ARNOLD et al., 1998; ARNOLD; FOHRER, 2005; WOFOST; DE WIT et al., 2019). These models enable simulating scenarios with distinct land management strategies, different environmental and climate conditions, and allow integration with other models (BETTS, 2005). However, although many of these models contain detailed process-based descriptions of involved processes, they implicitly are a simplification of the natural system, and include assumptions and generalizations in their structure and parameterization.

Among available hydrological models available, Richards-equation process-based agro-hydrological models provide detailed water and energy balances in the soil-water-atmosphere system with reliable results (VAN DAM et al., 2008). Nonetheless, they require large number of input parameters, especially those related to soil hydraulic properties, such as the water retention and unsaturated hydraulic conductivity functions. These parameters are prone to variation due to the hydraulic properties determination methods (LEKSHMI; SINGH; BAGHINI, 2014), related errors and uncertainties (HUPET; VAM DAM; VANCLOOSTER, 2004), and soil variability (HEUVELINK; WEBSTER, 2001), affecting agro-hydrological modelling results.

The soil hydraulic properties variability has been extensively studied by soil scientists, but only a few investigated uncertainty propagation of agro-hydrological model predictions (e.g., BARONI et al., 2010, BENNETT et al., 2013). Since the soil hydraulic properties determination are often very local and the number of replicates are limited, the characterization

of the spatial hydraulic properties may be misestimated and model predictions are vulnerable to errors. Therefore, model predictions should be interpreted considering both uncertainty of input parameters and hydraulic properties variability for more reliable interpretation of the water balance and crop yield in agro hydrological systems.

In order to obtain more insights in the soil hydraulic properties determination and the effect of its uncertainty on agro-modelling predictions, in this thesis we report the estimation of soil hydraulic properties by inverse modelling as an alternative to traditional laboratory methods using the HYDRUS 1-D (ŠIMŮNEK et al., 1998) (Chapter 2), and analyze the influence of the hydraulic properties uncertainties on the SWAP (KROES et al., 1998) predictions by uncertainty analysis.

In Chapter 2, the inverse modelling was performed to obtain hydraulic properties using water content data measured by Frequency Domain Reflectometry (FDR) sensors during six months at two depths in a small field experiment. Part of the monitoring period was used to calibrate Mualem-van Genuchten parameters and the remaining period was used to validate the modelling results comparing simulated water contents to observed ones. The HYDRUS 1-D was used to inversely estimate the Mualem-van Genuchten parameters and associated uncertainties, then further applied in uncertainty analysis of SWAP model predictions.

In chapter 3, the water balance components and crop yield were simulated for a 30 years period (1987–2017) for a rainfed maize crop growing every year from October 15 until March 15 by stochastic realizations of SWAP model. Two sampling methods were used to generate different sets of Mualem-van Genuchten parameters, one using standard errors obtained from the inverse modelling, and the other using the Latin Hypercube Sampling. A comparison between measured and simulated water contents was made.

Finally, considerations and general conclusion regarding agro-hydrological modelling were made in Chapter 4.

## References

- ARNOLD, J.G.; FOHRER, N. SWAT 2000: current capabilities and research opportunities in applied watershed modelling. **Hydrological Processes**, Chichester, v. 19, p. 563–572, 2005.
- ARNOLD, J.G.; SRINIVASAN, R.; MUTTIAH, R.; WILLIAMS, J. Large area hydrologic modeling and assessment. Part I: Model development. **Journal of the American Water Resources Association**, Philadelphia, v. 34, p. 73–89, 1998.
- BARONI, G.; FACCHI, A.; GANDOLFI, C.; ORTUANI, B.; HORESCHI, D.; VAN DAM, J.C. Uncertainty in the determination of soil hydraulic parameters and its influence on the performance of two hydrological models of different complexity. **Hydrological and Earth System Sciences**, Gottingen, v. 14, p. 251–270, 2010.
- BENNETT, S.J.; THOMAS, F.A.; BISHOP, R.; VERVOORT, W. Using SWAP to quantify space and time related uncertainty in deep drainage model estimates: A case study from northern NSW, Australia. **Agricultural Water Management**, Amsterdam, v. 130, n. C, p. 142–153, 2013
- BETTS, R.A. Integrated approaches to climate-crop modelling: Needs and challenges. **Philosophical Transactions of the Royal Society of London B**, London, v. 360, p. 2049-2065, 2005.
- DE WIT, A.; BOOGAARD, H.; FUMAGALLI, D.; JANSSEN, S.; KNAPEN, R.; VAN KRAALINGEN, D.; SUPIT, I.; VAN DER WIJNGAART, R.; VAN DIEPEN, K. 25 years of the WOFOST cropping systems model. **Agricultural Systems**, Amsterdam, v. 168, p. 154-167, 2019.
- JONES, C.A.; KINIRY, J.R. **CERES-Maize**: A simulation model of maize growth and development. College Station: Texas A&M University Press, 1986.
- KROES, J.G.; VAN DAM, J.C.; GROENENDIJK, P.; HENDRIKS, R.F.A.; JACOBS, C.M.J. **SWAP version 3.2**: Theory description and user manual. Wageningen: Alterra, 2008. 262 p. (Alterra Report, 1649).
- HEUVELINK, G.; WEBSTER, R. Modelling soil variation: Past, present, and future. **Geoderma**, Amsterdam, v. 100, n. 3-4, p. 269-301, 2001.
- HUPET, F.; VAN DAM, J.C.; VANCLOOSTER, M. Impact of within-field variability in soil hydraulic properties on transpiration fluxes and crop yields: A numerical study. **Vadose Zone Journal**, Madison, v. 3, p. 1367–1379, 2004.
- LEKSHMI, S.U.; SINGH, D.N.; SHOJAEI BAGHINI, M. A critical review of soil moisture measurement. **Measurement**, Amsterdam, v. 54, p. 92-105, 2014.
- PENNING DE VRIES, F.W.T.; JANSEN, D.M.; TEN BERGE, H.F.M.; BAKEMA, A. **Simulation of ecophysiological processes of growth in several annual crops**. Wageningen: Pudoc, 1989.

ŠIMŮNEK, J.; HUANG, K.; VAN GENUCHTEN, M.T. **The HYDRUS code for simulating the one-dimensional movement of water, heat, and multiple solutes in variably-saturated media**. Riverside: U.S. Salinity Laboratory, 1998. 164 p. (Research Report, 144).

VAN DAM, J.C.; GROENENDIJK, P.; HENDRIKS, R.F.A.; KROES, J.G. Advances of modeling water flow in variably saturated soils with SWAP. **Vadose Zone Journal**, Madison, v. 7, n. 2, p. 640-653, 2008.

VANCLOOSTER, M.; VIAENE, P.; CHRISTIAENS, K.; DUCHEYNE, S. **WAVE: A mathematical model for simulating water and agro-chemicals in the soil and vadose environment**. Reference and user's manual. Leuven: Institute for Land and Water Management, Katholieke Universiteit, 1996.

VERECKEN, H. et al. Modeling soil processes: review, key challenges, and new perspectives. **Vadose Zone Journal**, Madison, v. 15, n. 5, p. 1-57, 2016.

## 2 DETERMINING HYDRAULIC PROPERTIES OF A TROPICAL SOIL BY INVERSE MODELLING OF FIELD WATER CONTENTS

### Abstract

Soil water retention and hydraulic conductivity functions are most commonly determined by laboratory experiments with a pressure device based on hydrostatic equilibrium. However, these methods may be questioned with respect to sample representativeness and the validity of the equilibrium between soil sample and device. As an alternative, inverse modelling of transient conditions has been applied to estimate soil hydraulic properties. In this paper, we aimed to analyze the suitability of inverse modelling to estimate soil hydraulic properties using water content data obtained with FDR sensors in a field experiment, and compare these results with laboratory method. Our results showed that the Mualem-van Genuchten parameters  $n$  and  $K_s$  from both horizons were estimated with low accuracy by inverse modelling. Possibly, water content data used for inverse modelling did not provide enough information to estimate these parameters with high accuracy. Low values of water content found in the field in the A horizon led to a lower estimate of  $\theta_r$  compared to the laboratory method which is limited to 15000 cm of suction. In the Bt horizon, the small observed range of field water contents contributed to unreliable estimation of parameters  $\theta_r$  and  $n$ .  $K_s$  estimation for both horizons was negatively affected when using a fixed value for the tortuosity exponent ( $\lambda = 0.5$ ). Substituting some of the parameters by known or measured values together with a wider range of observed water contents or matric potentials may improve parameter estimation. Hydraulic modelling based on the Richards equation using inverse modelling led to apparently more reliable results than traditional laboratory methods. This is especially the case for the surface layer subject to atmospheric evaporative demand that may lead to air-dry values.

Keywords: Soil hydraulic properties. Inverse modelling. Ferralic Nitisol. HYDRUS 1-D.

### 2.1 Introduction

Temporal and spatial prediction of unsaturated flow in soils using the Richards equation relies on the soil hydraulic functions, specifically water content ( $\theta$ ) and unsaturated hydraulic conductivity ( $K$ ) versus matric potential ( $h$ ). Whereas soil hydraulic properties may be predicted from texture and other available soil survey information using pedotransfer functions, these functions contain a high level of statistical uncertainty (VERECKEN et al., 2010). Therefore measurement of hydraulic properties is, when possible, preferred.

The most common way to determine the soil water retention curve (SWRC) is from outflow experiments by establishing a hydrostatic equilibrium using a pressure plate extractor or hanging water column. Although widely used, results obtained by these methods should be interpreted with care, as they have their limitations. In the first place, soil samples may not be representative of field conditions. To represent the respective soil layer, samples should be undisturbed. In practice, this is hard to be accomplished. Furthermore, any sampling strategy

deals with matters related to representativeness and spatial variability (MITTELBACH; SENEVIRATNE, 2012).

Establishing a real hydrostatic equilibrium poses another challenge to these methods. It may take months before such an equilibrium is established between a pressure or suction device and the soil sample, especially at high pressures for fine-textured soils (BITTELLI; FLURY, 2009; GUBIANI et al., 2012). Moreover, field samples are under overburden pressure, whereas soil samples are not. This may result in an unnatural swelling of the soil sample (SOLONE et al., 2012). In laboratory outflow experiments, high pressure gradients are established when a large suction is applied on a saturated soil sample, whereas in field conditions, contrarily, large pressure gradients occur when the soil is moistened from a dry condition (VAN DAM; STRICKER; DROOGERS, 1994). These facts make the results from laboratory outflow experiments sometimes unreliable or not representative for field soil conditions.

In the last decades, inverse modelling has been used as an alternative to the traditional laboratory methods to overcome some of these problems (KOOL; PARKER; VAN GENUCHTEN, 1985). Finite difference numerical methods are not restricted by simplifications to solve the Richards equations and allow the use of flexible boundary and initial conditions (VAN DAM; STRICKER; DROOGERS, 1994). This approach enables a rapid and cost-effective soil hydrological characterization with high reliability (VRUGT et al., 2004) and hydraulic properties uncertainties can readily be assessed. Additionally, both retention and hydraulic conductivity functions can be estimated simultaneously from transient flow data.

However, the inverse solution of Richards equation has its drawbacks. The nonlinearity of soil hydraulic functions makes the parameter optimization a complex computational task. The correlation of hydraulic parameters and the nonuniqueness of the inverse solution may lead to a non-representative set of hydraulic parameters, especially when a large number of parameters are estimated at the same time (ŠIMŮNEK; VAN GENUCHTEN; SEJNA, 2012). Convergence is another issue, as nonlinear optimization often does not converge at first attempt and further investigation to detect inaccuracies is needed.

The suitability of inverse modelling for hydraulic properties estimation relies on issues which directly affect the well posedness of the solution: type of transient experiment and kind of initial and boundary conditions (ŠIMŮNEK; VAN GENUCHTEN, 1996); quality of data in terms of appropriate quantity and informative observational data (ECHING; HOPMANS, 1993); appropriate model to describe soil hydraulic properties (ZURMÜHL; DURNER, 1998); construction of multiple sources of information in an objective function (VAN DAM;

STRICKER; DROOGERS, 1994) and, the optimization algorithm used to find the global minimum and uncertainties associated to estimated parameters (VRUGT et al., 2003).

In many studies, numerical solution of the Richards equation in laboratory experiments have been applied with good results (VAN DAM.; STRICKER; DROOGERS, 1992; 1994; ECHING; HOPMANS, 1993; ŠIMŮNEK; VAN GENUCHTEN, 1996; ARORA; MOHANTY; MCGUIRE, 2011; PINHEIRO; DE JONG VAN LIER; METSELAAR, 2017), however, applications in field experiments are more complex. Soil spatial variability and the uncertainties in boundary conditions have been the major concerns of this method (VRUGT et al., 2004; SCHARNAGL et al., 2011; MAVIMBELA; VAN RENSBURG, 2013; LE BOURGEOIS et al., 2016).

In this paper, we aimed to analyze the suitability of inverse modelling to estimate soil hydraulic properties at field scale using spatially distributed water content data measured in the field. We also compared the hydraulic properties derived from inverse modelling with those obtained by laboratory methods. Finally, we evaluate the capability of hydraulic properties derived from both methods to simulate surface and bottom flux using a Richards equation-based hydrological model.

## 2.2 Material and Methods

### 2.2.1 Site description

An experimental plot with an extension of 10 x 25 m (230 m<sup>2</sup>) was used in Piracicaba/Brazil (22° 42' 26" S; 47° 37' 22" W). Within the plot, ten sites were chosen for soil hydraulic characterization (Figure 2.1). The area had previously been cultivated with *Brachiaria sp.*, but during the experiment it was maintained without vegetation. Results from Site #2 were eliminated from the analysis, as it appeared to contain a compacted spot with diverging hydraulic properties. The soil of the area is classified as a Ferralic Nitisol (IUSSWORKING GROUP WRB, 2015). Information about some soil characteristics is found in Table 2.1.

Figure 2.1 Schematic representation of the area with the 9 studied sites. Each site contains FDR sensors at its center (cross) for water content monitoring ( $\theta_f$ ), and four sampling locations in the corners for water retention characterization (dots) ( $n = 4$ ). Site #2 (in gray) was not used in this study

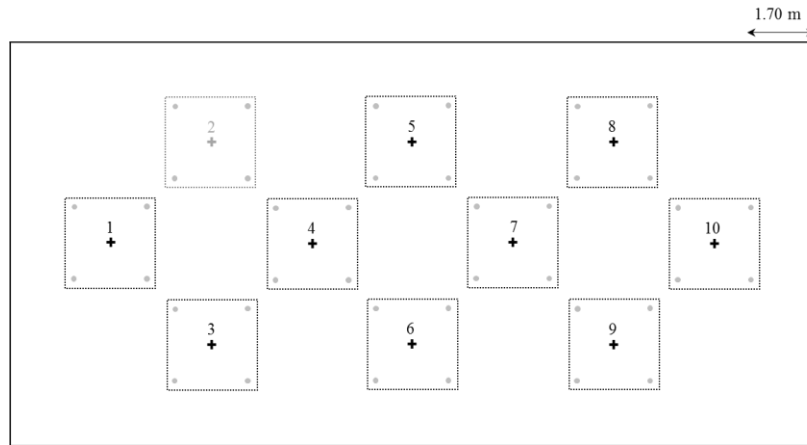
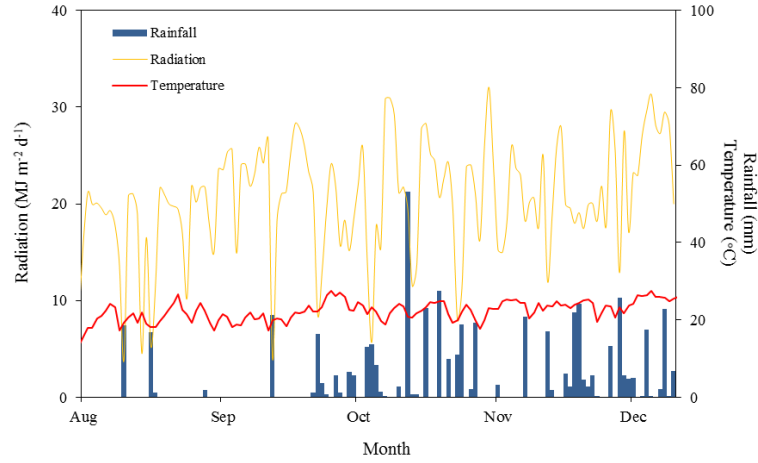


Table 2.1 Particle size distribution and particle density ( $\rho_p$ ) ( $n = 9$ ), bulk density ( $\rho_b$ ) ( $n = 36$ ), total porosity (TP, calculated from densities) ( $n = 36$ ), textural class, and type of structure for A and Bt horizons (mean values with standard deviations between brackets)

Horizon	Depth cm	Particle size distribution (mm)			$\rho_p$ kg m <sup>-3</sup>	$\rho_b$ kg m <sup>-3</sup>	TP m <sup>3</sup> m <sup>-3</sup>	Texture class	Type of structure
		Clay <0.002 mm	Silt 0.002-0.05 mm	Sand 0.05-2 mm					
		kg kg <sup>-1</sup>							
A	0 - 20	0.37 (0.03)	0.23 (0.05)	0.40 (0.05)	2932 (173)	1330 (123)	0.52	Clay Loam	Granular
Bt	20 - 40+	0.55 (0.02)	0.16 (0.04)	0.29 (0.05)	2971 (35)	1585 (89)	0.47	Clay	Blocky angular

Meteorological data including radiation, minimum and maximum temperature, vapor pressure, wind speed, and rainfall were obtained from the University of São Paulo weather station in Piracicaba/Brazil (22° 42' 10" S; 47° 37' 25" W, altitude 546 m), at about 500 m from the experimental area (Figure 2.2). The local climate is of the Koeppen Cwa type, with a dry winter from May to September.

Figure 2.2 Main daily rainfall, solar radiation and air temperature as observed at the University of São Paulo weather station in Piracicaba/Brazil during the period July - December 2016



### 2.2.2 Soil hydraulic parameterization

Soil hydraulic characterization of the nine sites of the experiment was performed using standard laboratory suction table and pressure plate extractor (in the following identified by LM), and by inverse modelling (identified by IM).

Soil hydraulic properties were described using the Van Genuchten (1980) equations with the Mualem restriction (MUALEM, 1976):

$$\Theta = \frac{\theta - \theta_r}{\theta_s - \theta_r} = \left[ 1 + |\alpha h|^n \right]^{1-n} \quad (2.1)$$

$$K(\theta) = K_s \Theta^\lambda \left[ 1 - (1 - \Theta^{\frac{n}{n-1}})^{1-\frac{1}{n}} \right]^2 \quad (2.2)$$

$$\Theta = \frac{\theta - \theta_r}{\theta_s - \theta_r} \quad (2.3)$$

where  $\theta$ ,  $\theta_r$  and  $\theta_s$  are water content, residual water content and saturated water content ( $\text{cm}^3 \text{cm}^{-3}$ ), respectively;  $h$  is matric potential (cm);  $\alpha$  ( $\text{cm}^{-1}$ ),  $n$  (-), and  $\lambda$  (-) are fitting parameters;  $K$  and  $K_s$  are hydraulic conductivity and saturated hydraulic conductivity, respectively ( $\text{cm d}^{-1}$ ).

### *Laboratory method (LM)*

Four undisturbed soil samples (5 cm diameter and 3 cm height) were collected at each of the 9 sites from A and Bt horizons, respectively at 0.00-0.10 and 0.30-0.40 m depths. In the laboratory, samples were saturated with an aqueous solution of 0.005 M of CaSO<sub>4</sub> by capillarity during 24h (DANE; HOPMANS, 2002).

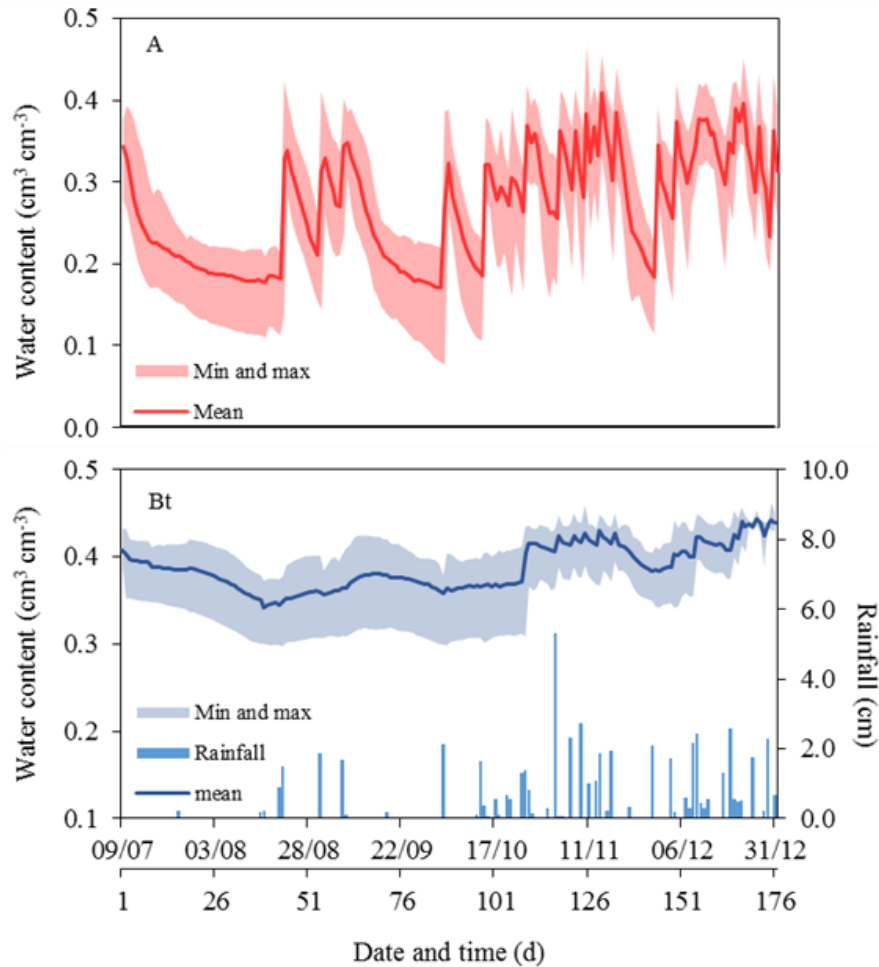
Water contents were determined after establishing equilibrium on a suction table ( $h = -10$  and  $-20$  cm) (TOPP; ZEBCHUK, 1979) and in a pressure plate extractor ( $h = -60, -100, -330, -1000, -3000,$  and  $-15000$  cm) (DANE; HOPMANS, 2002). The Mualem-van Genuchten equations were fitted to the measured water contents determining fitting parameters  $\theta_r$ ,  $\theta_s$ ,  $\alpha$  and  $n$ .

### *Inverse modelling (IM)*

Hydraulic parameters were estimated by inverse modelling using the hydrological model HYDRUS 1-D (ŠIMŮNEK et al., 1998). HYDRUS 1-D employs a Galerkin type linear finite element scheme to numerically solve the Richards equation. Additionally, the model has an inverse solution option to estimate soil hydraulic parameters performed by a Marquardt-Levenberg parameter optimization algorithm, which requires initial soil and boundary conditions.

The IM was performed using water content data from field measurement ( $\theta_f$ ) at 9 sites (Figure 2.1) in each horizon at depths 0.10 and 0.30 m. Water content was monitored every 15 minutes between July, 9 and December, 31 2016 (176 days) (Figure 2.3), by Frequency Domain Reflectometry (FDR) sensors (EC-5, Decagon Devices Inc.) with an accuracy of  $\pm 0.03 \text{ cm}^3 \text{ cm}^{-3}$  and a resolution of  $0.001 \text{ cm}^3 \text{ cm}^{-3}$ . The calibration equation provided by the manufacturer performs well in mineral soils and was used in this study (VAZ et al., 2013).

Figure 2.3 Mean daily water contents for A and Bt horizons from all sites of the experiment ( $\theta_f$ ) ( $n = 9$ ) using FDR sensors (line), and daily rainfall. The colored area represents the minimum and maximum water contents



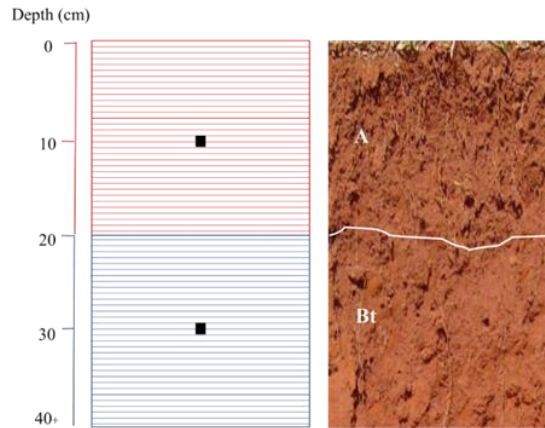
Data from July 9 to October 8 (a period of 92 days) were used to calibrate the hydraulic parameters. The second part of the experiment, from October 9 to December 31 (84 days), was used to validate the modelling results comparing simulated water contents ( $\theta_{sim}$ ) to observed ones. The calibration period coincided with the dry season (March to October), characterized by a few rainfall events. The validation period is part of the wet season (October to March).

For modelling purposes, the vertical soil profile was discretized into 40 nodes (Figure 2.4) and boundary conditions were set in terms of (1) potential surface evaporation flux ( $\text{cm d}^{-1}$ ) estimated using the Penman-Monteith equation (ALLEN et al., 1998; RITCHIE, 1972); (2) measured daily rainfall data from the weather station (upper boundary) (Figure 2.2); and (3) free drainage ( $\partial h/\partial z = 1$ ) (bottom boundary). The first water content measurement was used as

initial condition and different sets of Mualem-van Genuchten parameters were tested to start the IM procedure.

In our study, 10 parameters were estimated for each location, i.e.,  $\theta_r$ ,  $\theta_s$ ,  $n$ ,  $\alpha$  and  $K_s$  for both horizons. Parameter  $\lambda$  was assumed equal to 0.5 (MUALEM, 1976; VAN GENUCHTEN, 1980).

Figure 2.4 One-dimensional soil profile discretization with 40 nodes used in HYDRUS 1-D, showing soil horizons (A: red and B: blue) and sensor positions (squares)



### 2.2.3 Model performance evaluation

To evaluate the HYDRUS 1 D model performance, statistical indicators were calculated to compare observed and simulated water contents at each site: the coefficient of determination ( $r^2$ -eq. 2.4), Root Mean Square Error (RMSE-eq. 2.5), and the Nash-Sutcliffe efficiency coefficient (NSE-eq. 2.6) were used.

$$r^2 = \frac{\left[ \sum w_i \theta_i \hat{\theta}_i - \frac{\sum \theta_i \sum \hat{\theta}_i}{\sum w_i} \right]^2}{\left[ \sum w_i \theta_i^2 - \frac{(\sum \theta_i)^2}{\sum w_i} \right] \left[ \sum \hat{\theta}_i^2 - \frac{(\sum \hat{\theta}_i)^2}{\sum w_i} \right]} \quad (2.4)$$

$$RMSE = \sqrt{\frac{\sum_{i=1}^n (\theta_i - \hat{\theta}_i)^2}{n - m}} \quad (2.5)$$

$$NSE = 1 - \frac{\sum_{i=1}^n (\theta_i - \hat{\theta}_i)^2}{\sum_{i=1}^n (\theta_i - \bar{\theta}_i)^2} \quad (2.6)$$

where  $w_i = 1/\text{variance of measurement error of } \theta_i$ ,  $\theta_i$  and  $\hat{\theta}_i$  are observed and estimated water contents at time  $i$ , respectively,  $n$  is the number of observations, and  $m$  is the number of optimized parameters. The statistical model evaluation ratings for  $r^2$  and NSE are presented in Table 2.2 (MORIASI et al., 2015).

Table 2.2 Statistical model evaluation performance rating for coefficient of determination ( $r^2$ -eq. 2.4), and Nash-Sutcliffe efficiency (NSE-eq 2.6) (MORIASI et al., 2015)

Performance rating	$r^2$	NSE
Very good	> 0.85	> 0.80
Good	0.85 - 0.75	0.80 - 0.70
Satisfactory	0.75 - 0.60	0.7 - 0.50

## 2.3 Results and Discussion

### 2.3.1 Soil hydraulic parametrization

#### *Laboratory method*

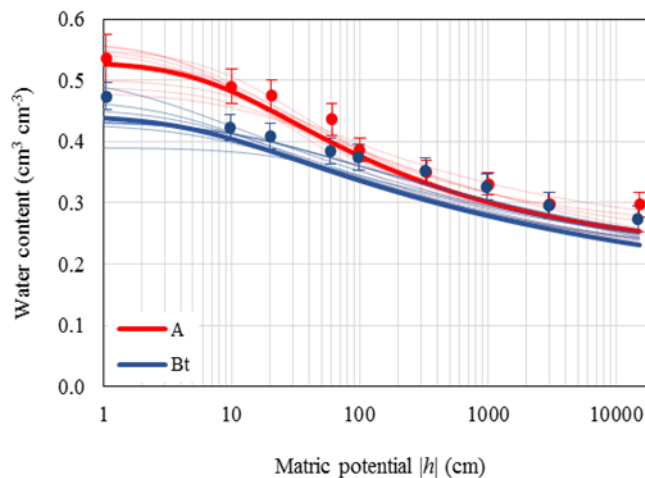
Mualem-van Genuchten model fitted well to measured data ( $r^2 \geq 0.95$ ). The corresponding hydraulic parameters and statistical indicators are presented in Table 2.3, measured and fitted SWRC for A and Bt horizons are shown in Figure 2.5.

In our experiment, the root system of *Brachiaria sp.* grown in the area before the experiment associated with land use may have played a role on the soil structure and hydraulic properties near saturation, contributing for higher soil total porosity (BEVEN; GERMANN, 2013). In contrast, this influence is not so pronounced in the subsurface, promoting less variability in the wet range of the Bt horizon (Figure 2.5).

Table 2.3 Mualem-van Genuchten fitting parameters and their descriptive statistics for A and Bt horizons for the laboratory method (LM) and inverse modelling (IM) (standard deviation between brackets)

Descriptive statistics	LM				IM				
	$\theta_r$	$\theta_s$	$\alpha$	$n$	$\theta_r$	$\theta_s$	$\alpha$	$n$	$K_s$
	$\text{cm}^3 \text{cm}^{-3}$	$\text{cm}^3 \text{cm}^{-3}$	$\text{cm}^{-1}$	(-)	$\text{cm}^3 \text{cm}^{-3}$	$\text{cm}^3 \text{cm}^{-3}$	$\text{cm}^{-1}$	(-)	$\text{cm d}^{-1}$
A Horizon									
Mean	0.21 (0.03)	0.53 (0.03)	0.117 (0.041)	1.26 (0.06)	0.06 (0.04)	0.42 (0.04)	0.084 (0.061)	1.67 (0.11)	10.40 (9.81)
Median	0.22	0.55	0.094	1.25	0.05	0.41	0.090	1.67	9.62
Min	0.15	0.48	0.069	1.15	0.00	0.37	0.020	1.49	1.91
Max	0.25	0.56	0.179	1.34	0.11	0.48	0.190	1.87	33.25
Bt Horizon									
Mean	0.14 (0.06)	0.44 (0.03)	0.180 (0.159)	1.15 (0.05)	0.18 (0.06)	0.42 (0.03)	0.015 (0.010)	1.26 (0.06)	14.94 (14.24)
Median	0.15	0.43	0.157	1.14	0.19	0.42	0.018	1.26	10.40
Min	0.04	0.39	0.026	1.09	0.08	0.37	0.003	1.17	4.16
Max	0.20	0.51	0.568	1.26	0.25	0.47	0.033	1.37	49.48

Figure 2.5 Soil water retention curves obtained by the laboratory method (LM) (points with standard deviation) and fitted by Mualem-van Genuchten model for A and Bt horizons for each site of the experiment ( $n = 9$ ). Bold lines represents the mean curve for each horizon ( $n = 9$ ), thin lines represent the mean of four replicates per site ( $n = 4$ )



For both horizons, parameter  $\alpha$  presented large standard deviation. This parameter represents a scaling factor of the matric potential and its determination is essential for soil water retention characterization. In the Bt horizon, the standard deviation of  $\alpha$  was the highest (Table 2.3), being of the same order of magnitude as the parameter itself (0.159 and 0.180  $\text{cm}^{-1}$ , respectively), indicating a doubtful determination of this parameter.

Parameter  $\theta_r$  and  $\theta_s$  presented a standard deviation of around 0.03  $\text{cm}^3 \text{cm}^{-3}$ , but twice as high for  $\theta_r$  in the Bt horizon (Table 2.3). Measurements in pressure chambers at high pressure may be doubtful due to non-equilibrium, leading to overestimating of corresponding water

contents. This may be caused by the loss of hydraulic contact between the ceramic pressure plate and the soil sample, or by hydraulic discontinuities within the soil sample, making the water release very slow. At the same time, the pressure in the chamber is maintained with compressed (hence: water saturated) air, possibly retarding a final equilibrium. Several studies demonstrated discrepancy in water contents comparing pressure plate extractor and vapor equilibrium methods when high suctions were applied. In those studies, higher water contents from pressure plate extractor determinations have been reported (CRESSWELL; GREEN; MCKENZIE, 2008; BITTELLI; FLURY, 2009; SCHELLE et al., 2013).

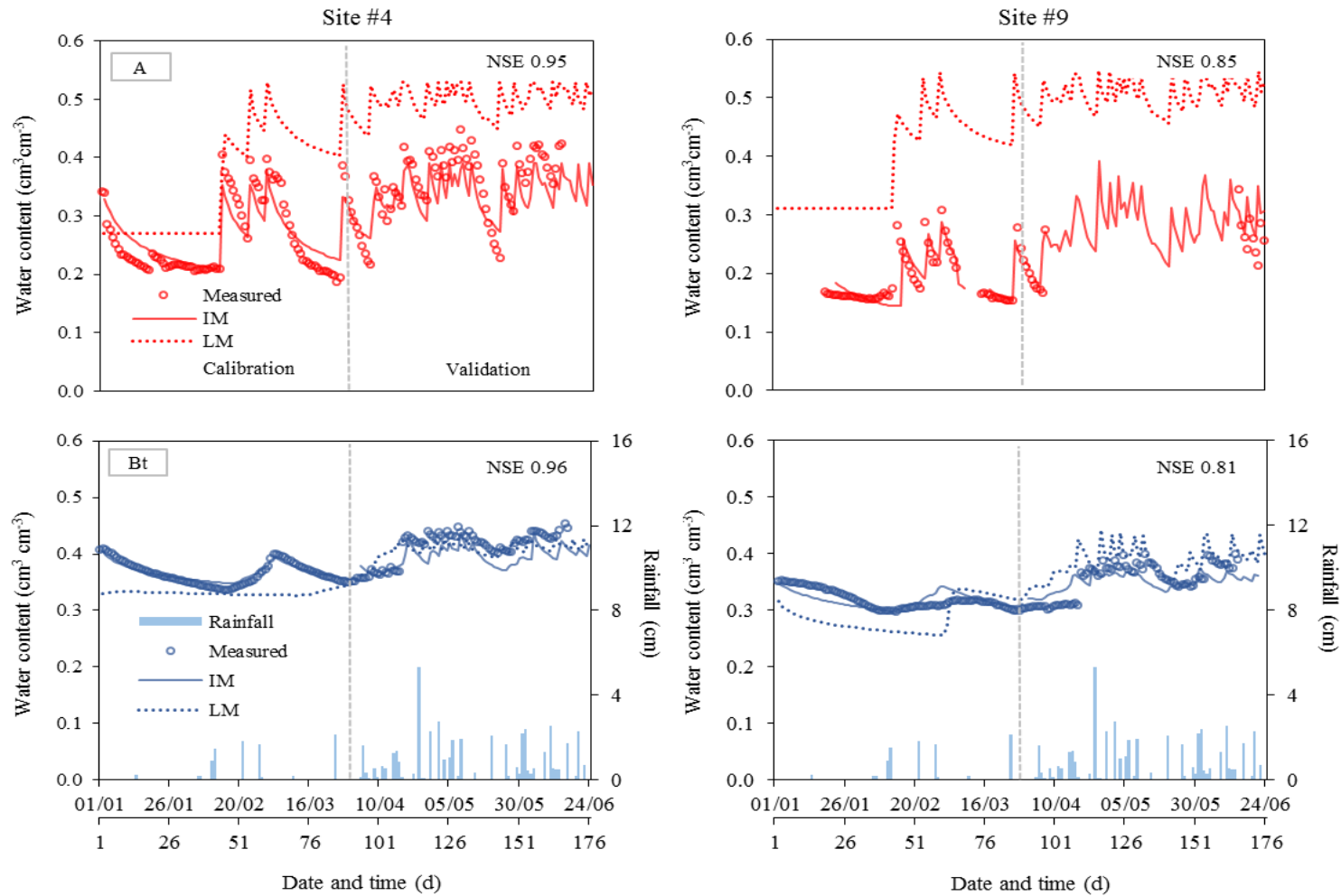
Therefore, the determination of  $\theta_r$  is merely a numerical extrapolation, which does not necessarily describe the retention properties beyond 15000 cm of suction. When obtained from extrapolation,  $\theta_r$  is a fitting parameter without clear physical meaning and positive and negative values can be obtained from unbiased SWRCs, even with very good fitting. To solve that problem, modified van Genuchten functions have been proposed to fit data in the dry part of the SWRC (ROSS; WILLIAMS; BRISTOW, 1991; GROENEVELT; GRANT, 2004). These equations inevitably require additional fitting parameters and present multiple inflection points.

### *Inverse modelling*

Measured and simulated water contents are shown in Figure 2.6 as a function of time for A and Bt horizons. The A horizon showed lower water contents because contrarily to the subsoil, the topsoil is subject to the atmospheric evaporative demand. The temporal variation of water content is remarkable in the A horizon, with a quick response to rainfall events and rapidly losing water after a few days, whereas the increase of water content in the subsoil is delayed.

The water content in the Bt horizon is relatively constant even in the dry periods (days 1 to 100) with a slight increase during the wet period (days 100 to 176). The variation of water content is lower in this horizon, with a minimum of  $0.08 \text{ cm}^3 \text{ cm}^{-3}$  and maximum of  $0.12 \text{ cm}^3 \text{ cm}^{-3}$ ; meanwhile, this is higher in the A horizon, with minimum of  $0.16 \text{ cm}^3 \text{ cm}^{-3}$  and maximum of  $0.33 \text{ cm}^3 \text{ cm}^{-3}$ .

Figure 2.6 Measured (dots) and simulated (lines) water contents performed with the Mualem-van Genuchten parameters for A and Bt horizons obtained using the laboratory method (LM) and inverse modelling (IM) over time for high and low NSE (Site #4 and Site #9, respectively) obtained by the inverse modelling



The HYDRUS 1-D calibration for both horizons was performed during the dry period (first 92 days of monitoring). The calibrated set of Mualem-van Genuchten parameters was then used to validate the model using data of the wet period (remaining 84 days). Mualem-van Genuchten estimated parameters along with standard error (95% confidence interval) are shown in Table 2.4. The model well described the water content over time with relatively high accuracy for Bt horizon, and somewhat lower accuracy for the A horizon (Figure 2.6 and Figure 2.7).

The hydraulic parameter estimation presented low precision (high standard errors) for  $n$  and  $K_s$  for both horizons, and for  $\theta_r$  for the Bt horizon (Table 2.4). In contrast, values of  $\theta_s$  and  $\alpha$  were reliable. The  $\theta_f$  data used in the calibration procedure may not have provided enough information for the model to estimate these parameters with high accuracy (STEENPASS et al., 2011), even in the A horizon which went through wetting and drying periods.

For the Bt horizon, the narrow range of  $\theta_f$  composed exclusively of high water content values contributed to an unreliable estimation of  $\theta_r$ . The low variation of  $\theta_f$  is also an important factor for inaccurate estimation of  $n$  for deeper horizons (GUBER et al., 2009) (Table 2.4). Measuring water contents over a wider range would improve their estimation, however, for the Bt horizon, low values for  $\theta_f$  may never be reached in field conditions.

Inverse modelling results can be improved by reducing the number of parameters to be estimated, and a common parameter to be fixed is  $\theta_s$ . The value of  $\theta_s$  to be used in this case is questionable. Total porosity calculated from bulk and particle density is an option, but sometimes field saturated water contents are 5 to 10% lower compared to laboratory measurements because of the entrapped air within the soil sample.

Saturated hydraulic conductivity  $K_s$  presented the lowest precision among all estimated parameters (Table 2.4). Parameter  $\lambda$  (eq. 2.2) was fixed ( $\lambda = 0.5$ ) with the aim to improve the estimation of  $K_s$ , but this apparently affected  $K_s$  estimation negatively. Apparently, field data did not contain enough information regarding hydraulic conductivity near saturation. As a solution,  $K_s$  could be determined independently (VAN DAM; STRICKER; DROOGERS, 1994) and the value of  $\lambda$  should then be estimated by inverse modelling.

Table 2.4 Estimated Mualem-van Genuchten parameters (eq. 2.1, eq. 2.2 and eq 2.3) and standard error for A and Bt horizons with model evaluation coefficients  $r^2$  and RMSE (95% confidence interval), and NSE for simulated water content ( $\theta_{sim}$ ) using hydraulic parameters provided by laboratory method (LM) and inverse modelling (IM) for all sites of the experiment

Site	Horizon	$\theta_r$	$\theta_s$	$\alpha$	$n$	$K_s$	$r^2$	RMSE	NSE	NSE
		$\text{cm}^3 \text{cm}^{-3}$		$\text{cm}^{-1}$	(-)	$\text{cm d}^{-1}$		$\text{cm}^3 \text{cm}^{-3}$	IM	LM
1	A	0.08 ± 0.02	0.48 ± 0.03	0.191 ± 0.022	1.73 ± 0.19	11.76 ± 3.29	0.96	0.01	0.77	0.55
	Bt	0.17 ± 0.08	0.44 ± 0.02	0.004 ± 0.002	1.31 ± 0.15	13.14 ± 6.35			0.81	0.83
3	A	0.02 ± 0.13	0.40 ± 0.07	0.026 ± 0.015	1.49 ± 0.38	12.78 ± 5.95	0.95	0.02	0.85	0.51
	Bt	0.10 ± 0.36	0.44 ± 0.02	0.007 ± 0.005	1.23 ± 0.26	4.16 ± 3.59			0.78	0.89
4	A	0.09 ± 0.04	0.39 ± 0.03	0.086 ± 0.028	1.73 ± 0.30	1.91 ± 0.98	0.89	0.02	0.95	0.83
	Bt	0.23 ± 0.17	0.45 ± 0.07	0.019 ± 0.009	1.37 ± 0.62	30.00 ± 21.39			0.96	0.92
5	A	0.11 ± 0.02	0.45 ± 0.05	0.092 ± 0.038	1.87 ± 0.43	33.25 ± 14.39	0.97	0.02	0.87	0.40
	Bt	0.20 ± 0.17	0.42 ± 0.01	0.015 ± 0.008	1.18 ± 0.13	5.71 ± 4.21			0.79	0.79
6	A	0.05 ± 0.03	0.44 ± 0.03	0.111 ± 0.031	1.63 ± 0.17	14.33 ± 2.64	0.92	0.02	0.96	0.79
	Bt	0.17 ± 0.16	0.40 ± 0.06	0.033 ± 0.047	1.30 ± 0.33	10.40 ± 35.90			0.96	0.95
7	A	0.10 ± 0.03	0.41 ± 0.02	0.164 ± 0.058	1.70 ± 0.22	4.54 ± 2.57	0.93	0.02	0.85	0.59
	Bt	0.25 ± 0.28	0.40 ± 0.01	0.023 ± 0.035	1.17 ± 0.29	7.33 ± 4.17			0.81	0.81
8	A	0.00 ± 0.12	0.37 ± 0.07	0.023 ± 0.015	1.58 ± 0.66	2.58 ± 4.62	0.93	0.03	0.98	0.61
	Bt	0.25 ± 0.44	0.40 ± 0.05	0.005 ± 0.023	1.28 ± 0.6	7.27 ± 24.28			0.99	0.68
9	A	0.05 ± 0.03	0.40 ± 0.04	0.041 ± 0.009	1.67 ± 0.23	9.62 ± 3.37	0.96	0.01	0.85	0.64
	Bt	0.09 ± 0.16	0.38 ± 0.02	0.011 ± 0.007	1.24 ± 0.01	12.90 ± 7.53			0.81	0.84
10	A	0.00 ± 0.05	0.45 ± 0.07	0.033 ± 0.011	1.60 ± 0.24	2.82 ± 3.26	0.92	0.03	0.99	0.87
	Bt	0.20 ± 0.40	0.47 ± 0.07	0.018 ± 0.022	1.26 ± 0.56	24.11 ± 32.11			1.00	0.99

Other uncertainties for the inverse modelling include the prediction of soil evaporation, a complex nonlinear process involving water and vapor transport, energy, and mass transfer across an air boundary layer. Evaporation is still not well described by hydrological models and may affect model predictions (OR et al., 2013). Therefore, the evaporation rate determined by HYDRUS 1-D may not be representative of field conditions and could have impaired parameter optimization, especially for the soil surface where the interaction with atmosphere is most pronounced.

The correlation amongst hydraulic parameter poses another challenge to IM. This issue can be more complex if the correlation between horizons is high. In our study, the correlation between parameters was more pronounced in the A horizon, and five sites presented high

correlation between horizons (Table 2.5). For both horizons, a high correlation between parameters  $n$  and  $\theta_r$  may have contributed to the low accuracy of their estimation. The parameter correlation matrix may be useful for further studies as prior analysis to determine which parameter to estimate and the best observational dataset for the inverse modelling procedure (SCHARNAGL et al., 2011). This may reduce labor and time efforts and possibly avoid ill-posed problems.

Figure 2.7 Measured and simulated water contents for Site #4 and Site #9 (high and low NSE, respectively, obtained from the inverse modelling) performed with the Mualem-van Genuchten parameters obtained using (a) inverse modelling (IM) and (b) the laboratory method (LM) for A and Bt horizons

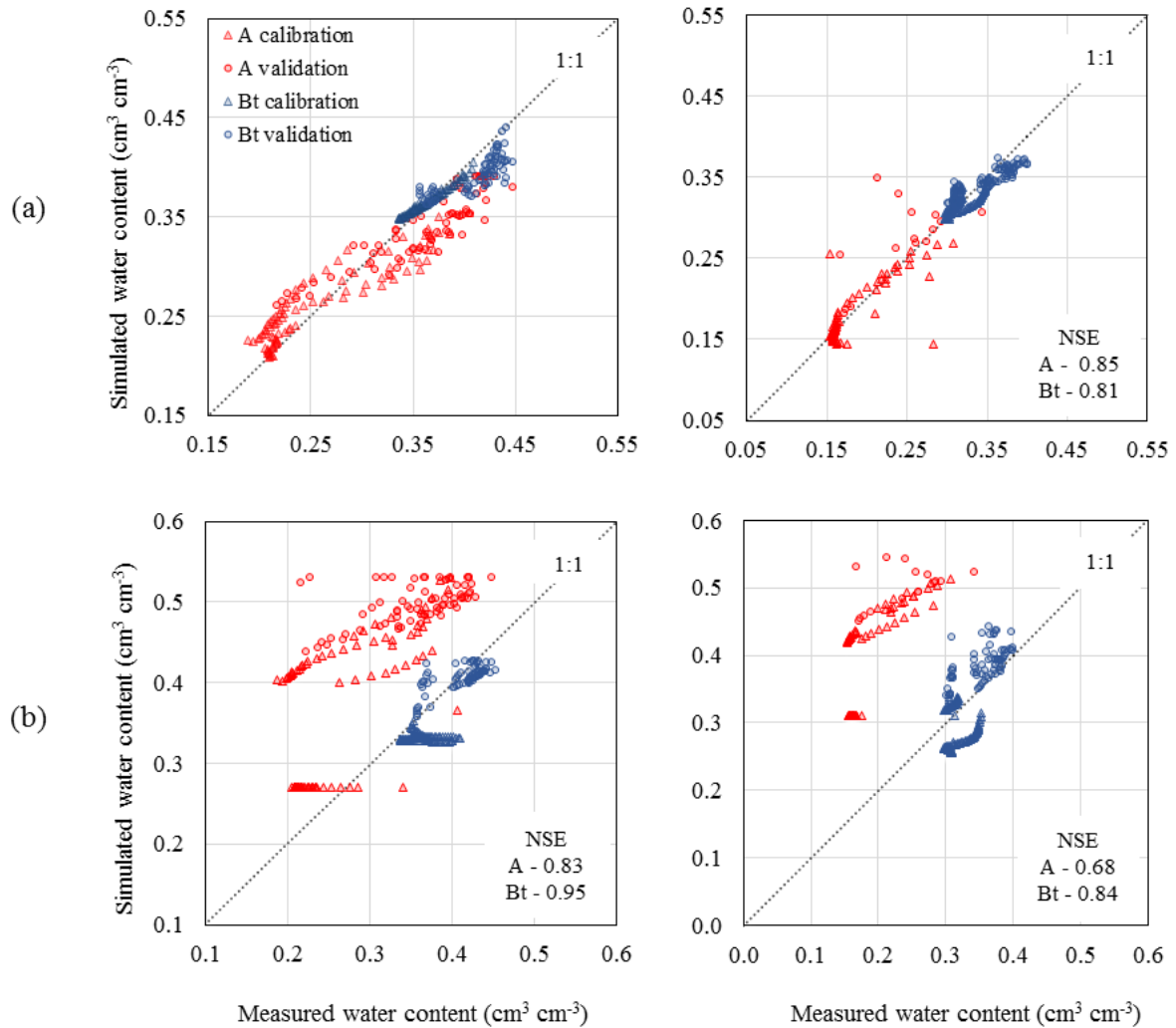


Figure 2.8 Measured water content ( $\theta_f$ ) and estimated matric potential ( $h_{est}$ ) using Mualem-van Genuchten parameters obtained by IM during the calibration period for A and Bt horizons for Site #10

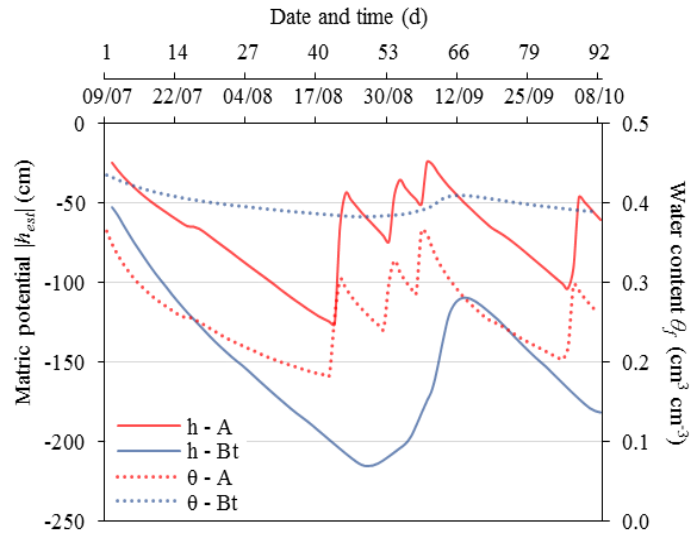


Table 2.5 Correlation coefficients between Mualem-van Genuchten parameters per horizon and between horizons. Red and blue colors represent the correlation between parameters for A and Bt horizons, respectively; black colors between Mualem-van Genuchten parameters from different horizons. Parameters without correlation are not shown. Correlations  $>0.6$  are indicated by bold numbers.

		A					Bt		A					Bt		A					Bt	
		$\theta_r$	$\theta_s$	$\alpha$	$n$	$K_s$	$\theta_r$	$\theta_s$	$\theta_r$	$\theta_s$	$\alpha$	$n$	$K_s$	$\theta_r$	$\theta_s$	$\theta_r$	$\theta_s$	$\alpha$	$n$	$K_s$	$\theta_r$	$\theta_s$
A	$\theta_s$	<b>0.67</b>	<b>1</b>						<b>0.34</b>	<b>1</b>						<b>0.52</b>	<b>1</b>					
	$\alpha$	-0.39	<b>-0.66</b>	<b>1</b>					-0.29	<b>-0.84</b>	<b>1</b>					-0.59	-0.40	<b>1</b>				
	$n$	<b>0.95</b>	<b>0.64</b>	-0.36	<b>1</b>				<b>0.87</b>	<b>0.66</b>	-0.56	<b>1</b>				<b>0.92</b>	<b>0.38</b>	-0.60	<b>1</b>			
	$K_s$	<b>0.16</b>	<b>0.76</b>	-0.52	0.02	<b>1</b>			-0.53	-0.51	<b>0.65</b>	<b>-0.75</b>	<b>1</b>			-0.44	<b>0.34</b>	<b>0.38</b>	<b>-0.69</b>	<b>1</b>		
Bt	$\theta_s$	-0.10	-0.05	-0.05	-0.07	-0.04	<b>0.52</b>	<b>1</b>	-0.03	<b>0.63</b>	<b>-0.63</b>	0.26	-0.36	<b>0.58</b>	<b>1</b>	0.22	-0.12	-0.14	0.35	-0.39	<b>0.90</b>	<b>1</b>
	$\alpha$	-0.07	-0.18	0.04	-0.12	-0.09	-0.56	-0.55	-0.14	-0.09	0.18	0.03	-0.12	<b>0.51</b>	<b>0.37</b>	0.08	0.09	-0.52	0.11	-0.14	-0.47	-0.43
	$n$	-0.04	0.09	-0.08	0.05	0.03	<b>0.96</b>	<b>0.67</b>	-0.05	0.42	-0.52	0.14	-0.26	<b>0.96</b>	<b>0.70</b>	0.26	-0.04	-0.16	0.36	-0.34	<b>0.98</b>	<b>0.96</b>
	$K_s$	-0.03	-0.15	0.06	-0.12	-0.07	-0.57	<b>0.06</b>	-0.04	-0.14	0.19	-0.13	0.14	-0.40	-0.09	-0.37	-0.44	0.28	-0.28	-0.05	-0.54	-0.45
A	$\theta_s$	<b>0.74</b>	<b>1</b>						<b>0.85</b>	<b>1</b>						<b>0.60</b>	<b>1</b>					
	$\alpha$	-0.39	-0.59	<b>1</b>					<b>-0.78</b>	<b>-0.73</b>	<b>1</b>					-0.56	-0.24	<b>1</b>				
	$n$	<b>0.91</b>	<b>0.92</b>	-0.56	<b>1</b>				<b>0.91</b>	<b>0.93</b>	<b>-0.86</b>	<b>1</b>				<b>0.94</b>	<b>0.39</b>	<b>-0.62</b>	<b>1</b>			
	$K_s$	-0.31	-0.20	<b>0.59</b>	-0.38	<b>1</b>			-0.37	-0.34	<b>0.71</b>	<b>-0.61</b>	<b>1</b>			-0.17	<b>0.63</b>	<b>0.32</b>	-0.45	<b>1</b>		
Bt	$\theta_s$	-0.37	-0.09	0.00	-0.24	0.02	<b>0.30</b>	<b>1</b>	0.02	0.05	-0.35	0.07	-0.20	<b>0.40</b>	<b>1</b>	-0.25	-0.18	0.14	-0.23	0.05	<b>0.77</b>	<b>1</b>
	$\alpha$	-0.41	0.02	-0.04	-0.15	0.12	<b>0.01</b>	<b>0.76</b>	-0.07	0.08	-0.36	0.17	-0.43	<b>0.41</b>	<b>0.54</b>	0.10	-0.03	-0.23	0.18	-0.16	<b>0.01</b>	-0.01
	$n$	0.21	0.09	-0.37	0.24	<b>-0.60</b>	<b>0.92</b>	<b>0.09</b>	0.11	0.17	-0.35	0.16	-0.18	<b>0.93</b>	<b>0.54</b>	-0.15	-0.09	0.07	-0.13	0.04	<b>0.98</b>	<b>0.87</b>
	$K_s$	-0.41	-0.13	0.23	-0.33	0.35	-0.18	<b>0.81</b>	0.24	0.16	-0.22	0.19	-0.07	-0.42	<b>0.00</b>	-0.34	-0.31	0.28	-0.29	-0.04	-0.53	-0.37
A	$\theta_s$	<b>0.77</b>	<b>1</b>						<b>0.36</b>	<b>1</b>						<b>0.51</b>	<b>1</b>					
	$\alpha$	<b>-0.63</b>	<b>-0.71</b>	<b>1</b>					<b>-0.84</b>	-0.18	<b>1</b>					<b>0.03</b>	<b>0.45</b>	<b>1</b>				
	$n$	<b>0.93</b>	<b>0.84</b>	<b>-0.73</b>	<b>1</b>				<b>0.95</b>	<b>0.24</b>	<b>-0.84</b>	<b>1</b>				<b>0.83</b>	<b>0.23</b>	-0.25	<b>1</b>			
	$K_s$	<b>0.21</b>	<b>0.50</b>	<b>0.04</b>	<b>0.06</b>	<b>1</b>			-0.57	<b>0.47</b>	<b>0.70</b>	<b>-0.70</b>	<b>1</b>			<b>0.19</b>	<b>0.88</b>	<b>0.67</b>	-0.20	<b>1</b>		
Bt	$\theta_s$	-0.42	-0.57	0.12	-0.46	-0.50	<b>0.81</b>	<b>1</b>	0.48	0.03	-0.59	<b>0.63</b>	-0.57	<b>0.56</b>	<b>1</b>	-0.18	-0.45	-0.41	-0.05	-0.48	<b>0.85</b>	<b>1</b>
	$\alpha$	-0.42	<b>-0.64</b>	0.19	-0.40	<b>-0.62</b>	<b>0.52</b>	<b>0.77</b>	0.58	-0.05	<b>-0.64</b>	<b>0.76</b>	<b>-0.68</b>	<b>0.80</b>	<b>0.82</b>	-0.11	<b>-0.69</b>	<b>-0.62</b>	0.30	<b>-0.82</b>	<b>0.24</b>	<b>0.53</b>
	$n$	-0.32	-0.35	0.01	-0.37	-0.24	<b>0.98</b>	<b>0.85</b>	0.28	0.34	-0.29	0.43	-0.12	<b>0.94</b>	<b>0.70</b>	-0.18	-0.20	-0.13	-0.18	-0.17	<b>0.99</b>	<b>0.89</b>
	$K_s$	-0.14	-0.47	0.20	-0.16	<b>-0.61</b>	<b>0.15</b>	<b>0.48</b>	<b>0.63</b>	-0.37	<b>-0.82</b>	<b>0.66</b>	<b>-0.92</b>	<b>0.14</b>	<b>0.48</b>	0.12	<b>-0.61</b>	-0.61	0.37	<b>-0.76</b>	-0.26	<b>0.08</b>

### 2.3.2 Model performance

The water content over time was simulated using the Mualem-van Genuchten parameters obtained from LM and IM. For LM simulations,  $K_s$  obtained from IM was used, and for both methods,  $\lambda = 0.5$  was applied.  $\theta_{sim}$  were remarkably different for the two methods. The hydraulic parameters obtained from IM described  $\theta_{sim}$  well, while hydraulic parameters obtained from LM presented low performance (Table 2.4 and Figure 2.6).

The simulation of water content using hydraulic parameters obtained from LM overestimated  $\theta_{sim}$  in the A horizon for all sites during the simulated period (Figure 2.7). In the Bt horizon,  $\theta_{sim}$  values were closer to  $\theta_f$ , however in some sites  $\theta_{sim}$  was misestimated during some part of the simulated period. Despite this difference,  $\theta_{sim}$  was simulated with higher accuracy in the Bt horizon, with NSE-values  $\geq 0.78$ . Meanwhile, the A horizon showed lower NSE values (Table 2.4). In the Bt horizon,  $\theta_{sim}$  prediction by LM was similar to IM for most of the sites.

The SWRCs derived from both methods are clearly different for the A horizon, while for the Bt horizon they presented similar shape (Figure 2.9). The Mualem-van Genuchten parameters were similar for the Bt horizon with exception of parameter  $\alpha$  which related to a flat shape in the wet range at suctions higher than 100 cm (Figure 2.9 and Figure 2.10). In the A horizon the SWRCs are clearly different, especially in the dry part. Higher  $\theta_r$ , associated with lower  $n$  values resulted in a flatter shape of the SWRCs for LM. The  $\theta_s$  values from LM were also higher as discussed previously.

The deviations in the SWRC obtained by both methods for the A horizon are due to the fact that  $\theta_f$  showed lower values than found in the LM. The range of determination of the hydraulic parameters was different for both methods; in the LM, the driest values refer to 15000 cm suction, whereas for the IM water contents reached air dry values (about 106 cm of suction). The lowest  $\theta$ -value found in the LM was  $0.27 \text{ cm}^3 \text{ cm}^{-3}$  obtained at 15000 cm of suction in the pressure plate extractor, whereas field values became as low as  $0.08 \text{ cm}^3 \text{ cm}^{-3}$  (Figure 2.11). Furthermore, more than half of the measured  $\theta_f$ -values corresponded to pressure heads more negative than  $h = -15000 \text{ cm}$ , which contributed to the differences in hydraulic parameter estimation, as shown in Figure 2.9. In the Bt horizon, the water content ranges were similar for both methods and no  $\theta_f$  values below  $h = -15000 \text{ cm}$  ( $0.27 \text{ cm}^3 \text{ cm}^{-3}$ ) were measured; resulting SWRCs were similar (Figure 2.9 and Figure 2.10).

Figure 2.9 Soil water retention curves derived from laboratory method (LM) and inverse modelling (IM) fitted by Mualem-van Genuchten model for A and Bt horizons for each site of the experiment ( $n = 9$ ). Bold lines represents the mean curve for each horizon ( $n = 9$ ), thin lines represent the mean of four replicates per site ( $n = 4$ )

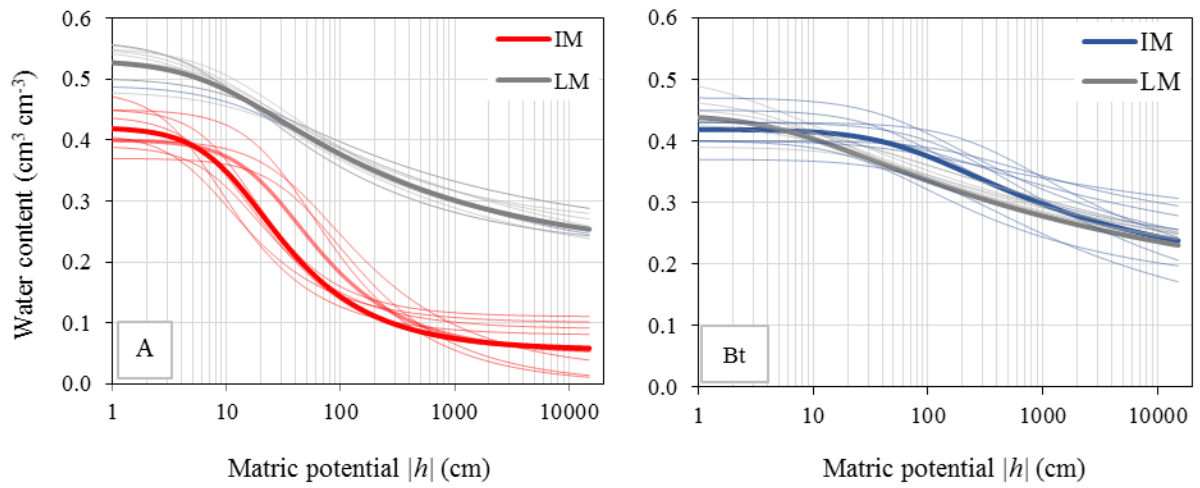


Figure 2.10 Mean Mualem-van Genuchten parameters obtained from laboratory method (LM) and inverse modelling (IM) for A and Bt horizons for all sites of the experiment ( $n = 9$ ). Each Mualem-van Genuchten parameter of LM represents the mean of four replicates ( $n = 4$ )

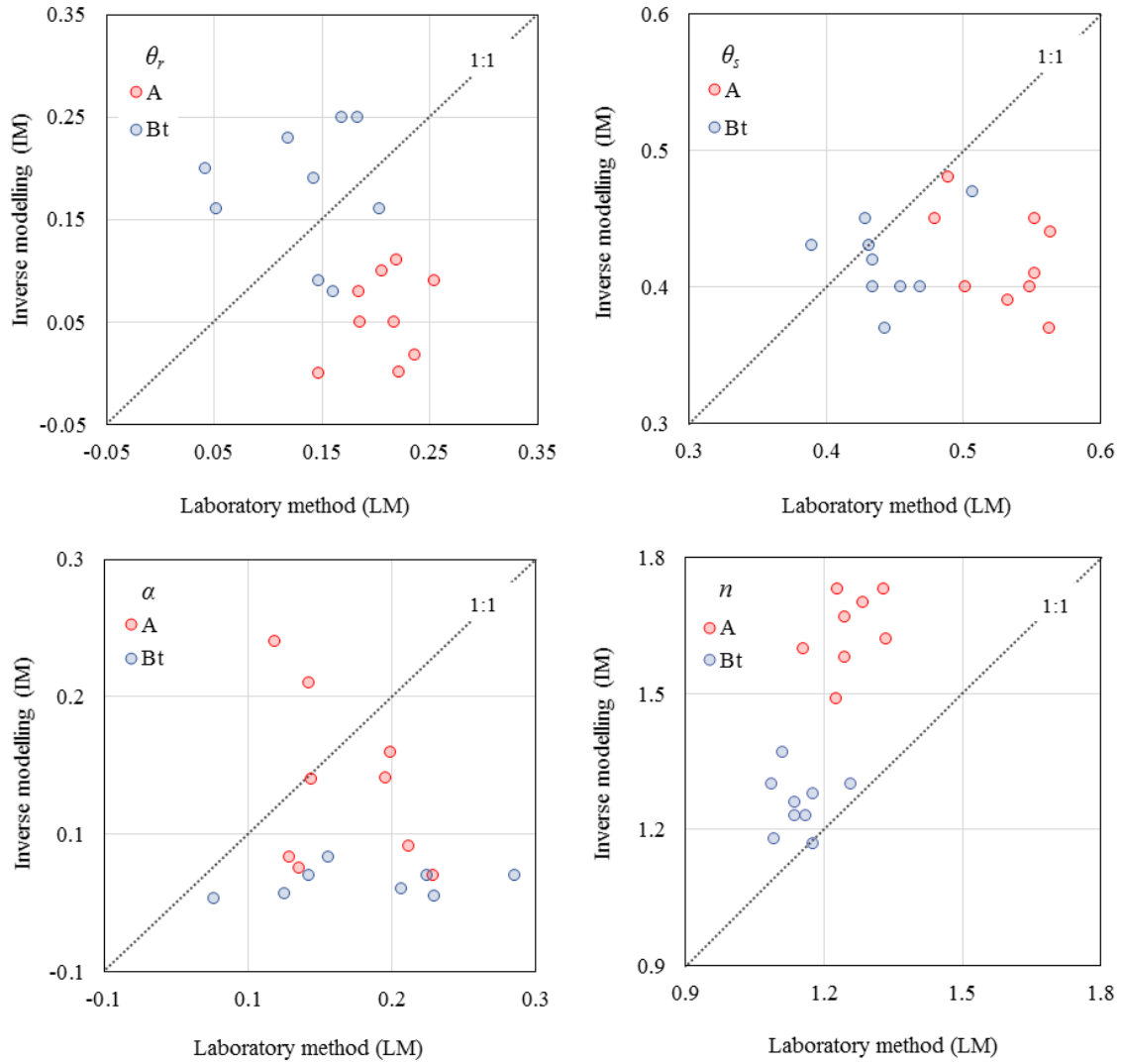
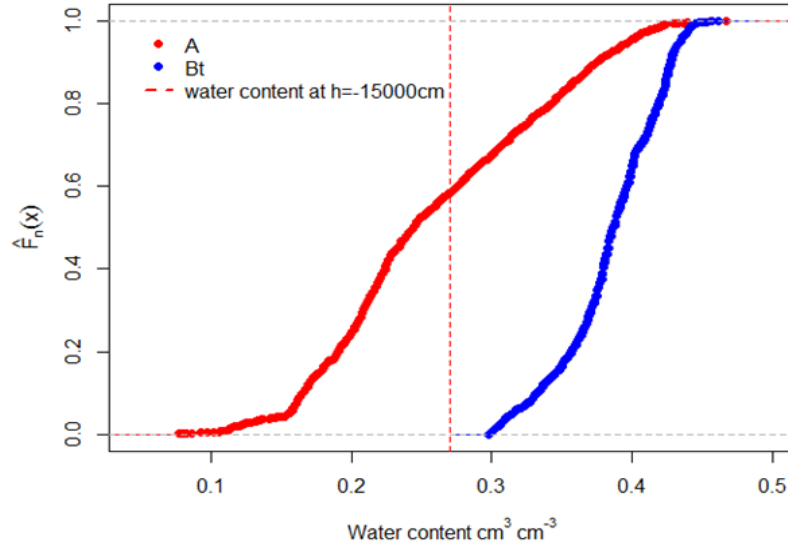


Figure 2.11 Empirical cumulative distribution function of water contents from field measurement ( $\theta_f$ ) for A and Bt horizons for all sites of the experiment ( $n = 9$ ). The dashed line represents water content ( $\theta$ ) at 15000 cm of suction for A and Bt horizons (lines are overlapped)



This poses the question of the LM, with pressure heads limited to the most negative value of 15000 cm, is adequate for simulation of drier conditions which may occur mainly near a soil surface due to evaporation. Besides this experimental issue, for these very low values of soil water content corresponding to very negative pressure heads, hydraulic functions based on the capillarity (BROOKS; COREY, 1964; VAN GENUCHTEN, 1980; KOSUGI, 1996; 1999), may not adequately describe very dry conditions where adsorption processes dominate retention properties (MADI et al., 2018).

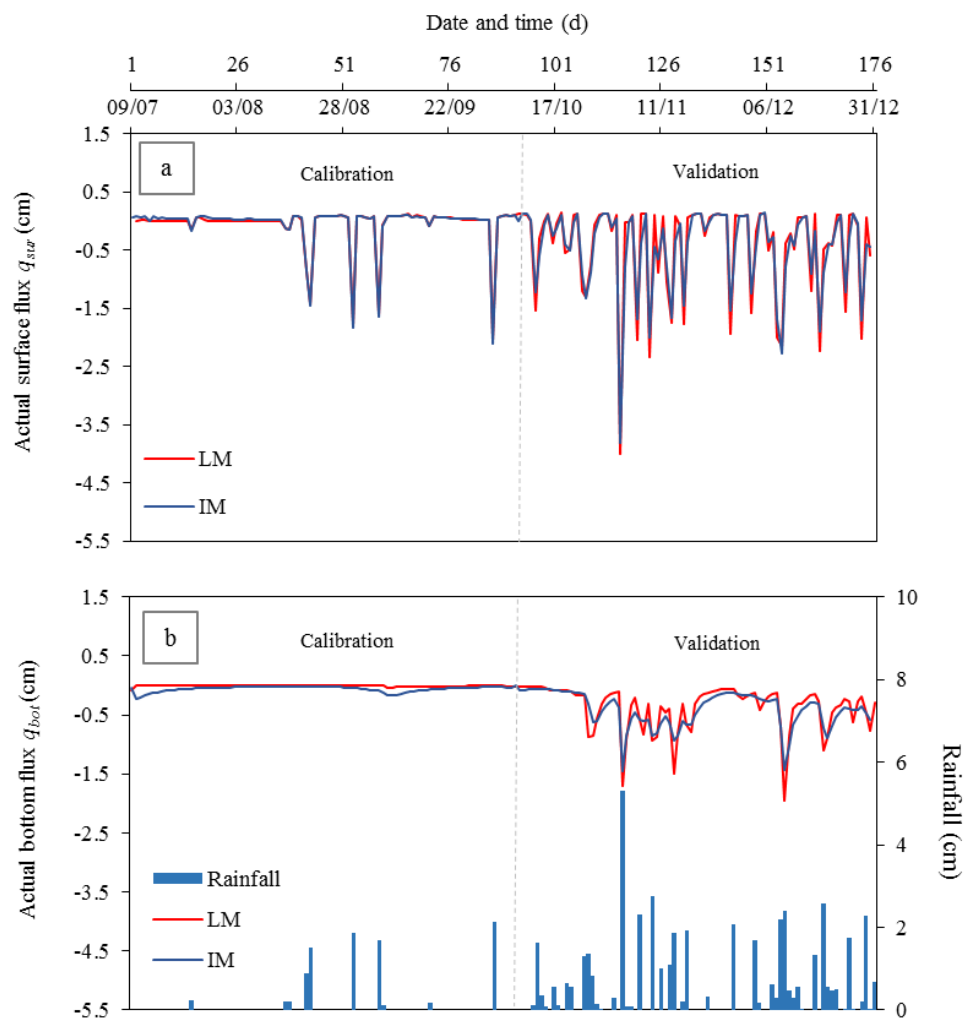
For this very dry range of the SWRC, some authors proposed retention functions based on adsorption processes (GROENEVELT; GRANT, 2004; LEBEAU; KONRAD, 2010; MADI et al., 2018), however, these functions are not implemented in most hydrological models. This is especially relevant in clay soils, where a substantial amount of water is released at matric potentials below  $h = -15000$  cm.

### 2.3.3 Actual surface ( $q_{sur}$ ) and bottom ( $q_b$ ) flux simulation

Mean simulated actual surface ( $q_{sur}$ ) and bottom flux ( $q_{bot}$ ) ( $\text{cm d}^{-1}$ ) are shown in Figure 2.12 using both LM and IM soil hydraulic parameters. Difference between the two methods is found mostly during the (wetter) validation period, especially for bottom flux. The  $q_{sur}$  simulation during the calibration period is similar for both methods. During the validation

period, parameters obtained from LM generated more intense inflow and outflow than IM. Hydraulic parameters from LM simulated  $q_{bot}$  near zero and did not predict much flux during the calibration period. The first rainfall events only wetted the soil profile for LM, whereas the simulation using parameters from IM generated outflow from the bottom of soil profile. During the validation period, parameters from LM generated more intense inflow and outflow than IM. The  $q_{bot}$  simulation shows that the set of hydraulic parameters derived from LM underestimated water flux during the dry period and provide more intense flux during the wet period. The set of hydraulic parameters chosen from each method affected surface and bottom flux simulation and, therefore, further water balance calculation.

Figure 2.12 Mean actual surface ( $q_{sur}$ ) (a) and bottom ( $q_{bot}$ ) (b) flux from all sites of the experiment ( $n = 9$ ) simulated by HYDRUS 1-D using Mualem-van Genuchten parameters obtained from laboratory method (LM) and inverse modeling (IM), and daily rainfall



## 2.4 Conclusions

Inverse modelling was performed with water content data from field measurement using FDR sensors. The Mualem-van Genuchten parameters were optimized using HYDRUS 1-D hydrological model for two horizons, resulting in good statistical indicators ( $r^2 \geq 0.89$  and  $RMSE \leq 0.03 \text{ cm}^3 \text{ cm}^{-3}$ ), but low accuracy for  $n$  and  $K_s$  estimation. For the Bt horizon, estimated  $\theta_r$  was not reliable.

We suggest two different approaches to improve the parameter optimization. First, less parameters should be estimated at the same location. This decreases the degree of freedom and provides a narrower confidence interval of the estimated parameters.  $\theta_s$  could be fixed and  $K_s$  could be measured independently, instead,  $\lambda$  could be included in the estimation. Second, water content monitoring in a wider range would add information and improve estimation precision. Additional information such as measured matric potential or soil evaporation may improve parameter estimation.

Hydraulic modelling based on Richards equation using inverse modelling led to more reliable results than laboratory methods. Water content determined from laboratory methods may contain errors derived from non-equilibrium within soil sample at high suctions. Moreover, these methods do not include very dry conditions because water content determination is generally limited to 15000 cm of suction. These limitations is especially important for the topsoil layer subjected to atmospheric evaporative demand that may reach air-dry values. These factors may cause discrepancy between water content determination from laboratory method and field conditions.

## References

- ALLEN, R.G.; PEREIRA, L.S.; RAES, D.; SMITH, M. **Crop evapotranspiration**. Guidelines for computing crop water requirements. Rome: FAO, 1998. (Irrigation and Drainage Paper, 56).
- ARORA, B.; MOHANTY, B.P.; MCGUIRE, J.T. Inverse estimation of parameters for multidomain flow models in soil columns with different macropore densities. **Water Resources Research**, Washington, v. 47, n. 4, W04512, 2011.
- BEVEN, K.; GERMANN, P. Macropores and water flow in soils revisited. **Water Resources Research**, Washington, v. 49, n. 3, p. 3071-3092, 2013.
- BITTELLI, M.; FLURY, M. Errors in water retention curves determined with pressure plates. **Soil Science Society of American Journal**, Madison, v. 73, n. 5, p. 1453–1460, 2009.
- BROOKS, R.H.; COREY, A.T. **Hydraulic properties of porous media**. Fort Collins, CO: Colorado State University, 1964. (Hydrology Paper, 3).

CRESSWELL, H.P.; GREEN, T.W.; MCKENZIE, N.J. The adequacy of pressure plate apparatus for determining soil water retention. **Soil Science Society of American Journal**, Madison, v. 72, n. 1, p. 41-49, 2008.

DANE, J.H.; HOPMANS, J.W. Pressure plate extractor. In: DANE, J.H., TOPP, G.C. (Ed.). **Methods of soil analysis**. Part 4. Physical methods. Madison: Soil Science Society of America, 2002. p. 671-720.

ECHING, S.O.; HOPMANS, J.W. Optimization of hydraulic functions from transient outflow and soil water pressure data. **Soil Science Society of American Journal**, Madison, v. 57, n. 3, p. 1167-1175, 1993.

GROENEVELT, P.H.; GRANT, C.D. A new model for the soil-water retention curve that solves the problem of residual water contents. **European Journal of Soil Science**, Oxford, v. 55, n. 3, p. 479-485, 2004.

GUBER, A.K.; PACHEPSKY, Y.A.; VAN GENUCHTEN, M.T.; ŠIMŮNEK, J.; JACQUES, D.; NEMES, A.; NICHOLSON, T.J.; CADY, R.E. Multimodel simulation on of water flow in a field soil using pedotransfer functions. **Vadose Zone Journal**, Madison, v. 8, n. 1, p. 1-10, 2009.

GUBIANI, P.I.; REICHERT, J.M.; CAMPBELL, C.; REINERT, D.J.; GELAIN, N.S. Assessing errors and accuracy in dew-point potentiometer and pressure plate extractor measurements. **Soil Science Society of American Journal**, Madison, v. 77, p. 19-24, 2012.

IUSS WORKING GROUP WRB. **World reference base for soil resources 2014: International soil classification system for naming soils and creating legends for soil maps**. Rome: FAO, 2015. 203 p. (World Soil Resources Reports, 106).

KOOL, J.B.; PARKER, L.C.; VAN GENUCHTEN, M.T. Determining soil hydraulic properties from one-step outflow experiment by parameter estimation: I. Theory and numerical studies. **Soil Science Society of American Journal**, Madison, v. 49, p. 1348-1354, 1985.

KOSUGI, K. Lognormal distribution model for unsaturated soil hydraulic properties. **Water Resources Research**, Washington, v. 32, n. 9, p. 2697-2703, 1996.

KOSUGI, K. General model for unsaturated hydraulic conductivity for soils with lognormal pore-size distribution. **Soil Science Society of American Journal**, Madison, v. 63, n. 2, p. 270-277, 1999.

LEBEAU, M.; KONRAD, J.-M. A new capillary and thin film flow model for predicting the hydraulic conductivity of unsaturated porous media. **Water Resources Research**, Washington, v. 46, W12554, 2010.

LE BOURGEOIS, O.; BOUVIER, C.; BRUNET, P.; AYRAL, P.-A. Inverse modelling of soil water content to estimate the hydraulic properties of a shallow soil and the associated weathered bedrock. **Journal of Hydrology**, Amsterdam, v. 541, pt. A, p. 116-126, 2016.

MADI, R.; DE ROOIJ, H.; MIELENZ, H.; MAI, J. Parametric soil water retention models: a critical evaluation of expressions for the full moisture range. **Hydrological and Earth System Sciences**, Gottingen, v. 22, n. 2, p. 1193–1219, 2018.

MAVIMBELA, S.S.D.; VAN RENSBURG, L.D. Estimating hydraulic conductivity of internal drainage for layered soils in situ. **Hydrological and Earth System Sciences**, Gottingen, v. 17, p. 4349–4366, 2013.

MITTELBACH, H.; SENEVIRATNE, S.I. A new perspective on the spatio-temporal variability of soil moisture: temporal dynamics versus time-invariant contributions. **Hydrological and Earth System Sciences**, Gottingen, v. 16, n. 7, p. 2169–2179, 2012.

MORIASI, D.N.; GITAU, M.W.; PAI, N.; DAGGUNPATI, P. Hydrologic and water quality models: Performance measures and evaluation criteria. **Transactions of the ASABE**, Saint Joseph, v. 58, n. 6, p. 1763–1785, 2015.

MUALEM, Y. A new model for predicting the hydraulic conductivity of unsaturated porous media. **Water Resources Research**, Washington, v. 12, n. 3, p. 513–522, 1976.

OR, D.; LEHMANN, P.; SHAHRAEENI, E.; SHOKRI, N. Advances in soil evaporation physics-A review. **Vadose Zone Journal**, Madison, v. 12, n. 4, p. 1–16, 2013.

PINHEIRO, E.A.R.; DE JONG VAN LIER, Q.; METSELAAR, K. A matric flux potential approach to assess plant water availability in two climate zones in Brazil. **Vadose Zone Journal**, Madison, v. 17, n. 1, p. 1–10, 2017.

RITCHIE, J.T. Model for predicting evaporation from a row crop with incomplete cover. **Water Resources Research**, Washington, v. 8, n. 5, p. 1204–1213, 1972.

ROSS, P.J.; WILLIAMS, J.; BRISTOW, K.L. Equation for extending water-retention curves to dryness. **Soil Science Society of American Journal**, Madison, v. 55, n. 4, p. 923–927, 1991.

SCHARNAGL, B.; VRUGT, J.A.; VEREECKEN, H.; HERBST, M. Inverse modelling of in situ soil water dynamics: investigating the effect of different prior distributions of the soil hydraulic parameters. **Hydrological and Earth System Sciences**, Gottingen, v. 15, n. 10, p. 3043–3059, 2011.

SCHELLE, H.; HEISE, L.; JÄNICKE, K.; DURNER, W. Water retention characteristics of soils over the whole moisture range: a comparison of laboratory methods. **European Journal of Soil Science**, Oxford, v. 64, n. 6, p. 814–821, 2013.

ŠIMŮNEK, J.; VAN GENUCHTEN, M.T. Estimating unsaturated soil hydraulic properties from tension disc infiltrometer data by numerical inversion. **Water Resources Research**, Washington, v. 32, n. 9, p. 2683–2696, 1996.

ŠIMŮNEK, J.; HUANG, K.; VAN GENUCHTEN, M.T. **The HYDRUS code for simulating the one-dimensional movement of water, heat, and multiple solutes in variably-saturated media**. Riverside: U.S. Salinity Laboratory, 1998. 164 p. (Research Report, 144).

ŠIMŮNEK, J.; VAN GENUCHTEN, M.T.; SEJNA, M. HYDRUS: Model use, calibration and validation. **Transactions of the ASABE**, Saint Joseph, v. 55, n. 4, p. 1261–1274, 2012.

SOLONE, R.; BITTELLI, M.; TOMEI, F.; MORARI, F. Errors in water retention curves determined with pressure plates: Effects on the soil water balance. **Journal of Hydrology**, Amsterdam, v. 470–471, n. 12, p. 65–74, 2012.

STEENPASS, C.; VANDERBORGHT, J.; HERBST, M.; ŠIMŮNEK, J.; VEREECKEN, H. Estimating soil hydraulic properties from infrared measurements of soil surface temperatures and TDR data. **Vadose Zone Journal**, Madison, v. 9, n. 4, p. 910–924, 2010.

TOORMAN, A.F.; WIERENGA, P.J.; HILLS, R.G. Parameter estimation of hydraulic properties from one step outflow data. **Water Resources Research**, Washington, v. 28, n. 11, p. 3021–3028, 1992.

TOPP, G.C.; ZEBCHUCK, W. The determination of soil water desorption curves for soil cores. **Canadian Journal of Soil Science**, Ottawa, v. 59, n. 1, p. 19–26, 1979.

VAN DAM, J.C.; STRICKER, J.N.M.; DROOGERS, P. Evaluation of the inverse method for determining soil hydraulic functions from one-step outflow experiments. **Soil Science Society of America Journal**, Madison, v. 56, n. 4, p. 1042–1050; 1992.

VAN DAM, J.C.; STRICKER, J.N.M.; DROOGERS, P. Inverse method for determining soil hydraulic functions from multi-step outflow experiments. **Soil Science Society of American Journal**, Madison, v. 58, n. 3, p. 647–652, 1994.

VAN GENUCHTEN, M.T. A closed-form equation for predicting the hydraulic conductivity of unsaturated soils. **Soil Science Society of American Journal**, Madison, v. 44, n. 5, p. 892–898, 1980.

VAZ, C.M.P.; JONES, S.; MEDING, M.; TULLER, M. Evaluation of standard calibration functions for eight electromagnetic soil moisture sensors. **Vadose Zone Journal**, Madison, v. 12, n. 2, p. 1–16, 2013.

VEREECKEN, H.; JAVAUX, M.; WEYNANTS, M.; PACHEPSKY, Y.; SCHAAP, M.G.; VAN GENUCHTEN, M.T. Using pedotransfer functions to estimate the van Genuchten–Mualem soil hydraulic properties: A Review. **Vadose Zone Journal**, Madison, v. 9, n. 4, p. 795–820, 2010.

VRUGT, J.A.; BOUTEN, W.; GUPTA, H.V.; HOPMANS, J.W. Toward improved identifiability of soil hydraulic parameters: On the selection of a suitable parametric model. **Vadose Zone Journal**, Madison, v. 2, n. 1, p. 98–113, 2003.

VRUGT, J.A.; SCHOUPS, G.; HOPMANS, J.W.; YOUNG, C.; WALLENDER, W.W.; HARTER, T.; BOUTEN, W. Inverse modelling of large-scale spatially distributed. Vadose zone properties using global optimization. **Water Resources Research**, Washington, v. 40, n. 6, W06503, 2004.

ZURMÜHL, T.; DURNER, W. Determination of parameters for bimodal hydraulic functions by inverse modelling. **Soil Science Society of American Journal**, Madison, v. 62, n. 4, p. 874–880, 1998.

### 3 HYDRAULIC PROPERTIES SAMPLING STRATEGIES AFFECT THE UNCERTAINTY OF VADOSE ZONE HYDROLOGICAL MODEL PREDICTIONS

#### Abstract

Uncertainty assessment of agro-hydrological model predictions provides information about the reliability of the model results which support water resources management and risk assessment. Among the different sources of uncertainty, the uncertainty related to soil hydraulic properties has a strong influence on the agro-hydrological model predictions. In this paper, we analyze the influence of the Mualem-van Genuchten parameters (M-VG) uncertainty on water balance components and crop yield predicted by the agro-hydrological SWAP for a soil under rainfed maize crop by uncertainty analysis using two Monte Carlo sampling methods. One method used Monte Carlo Random Sampling from normal distribution based on standard errors of the hydraulic parameters obtained from inverse modelling (MCRS), and the other used the Latin Hypercube Sampling (MCLHS). A deterministic simulation of SWAP using the mean of the M-VG parameters obtained from the inverse modelling was performed for comparison purposes. The validity of modelling results was assessed using simulated and water contents measured in the field. Our results showed that MCLHS and MCLHS generated distinct ranges and probability density distributions shape for the M-VG parameters and simulated results. The  $n$ -parameter was especially distinct for both horizons, and runoff ( $R_{off}$ ), soil evaporation ( $E_{soil}$ ) and bottom flux ( $q_{bot}$ ) showed remarkable differences between sampling methods. The M-VG parameters from MCRS may enhanced the uncertainty of simulated results, whereas MCLHS provided more reliable M-VG parameters combinations. The uncertainty analysis may provide useful information about the uncertainties of SWAP model predictions and should be preferred over a mere deterministic approach, which often provided results diverging those obtained from probabilistic methods. Moreover, the uncertainty analysis is a key tool for more reliable interpretation of the water balance and crop yield in agro hydrological systems and should be considered in agro modelling studies.

Keywords: Uncertainty analysis. Agro hydrological modelling. Latin Hypercube Sampling. SWAP model.

#### 3.1 Introduction

Agro hydrological models based on the Richards equation have been widely used to predict and simulate soil water balance components, solute transport, and crop yield under various conditions. These models provide detailed water and energy balances in the soil-water-atmosphere system with reliable results (VAN DAM et al., 2008). However, although many of these models contain detailed process-based descriptions of involved processes, they are a simplification of the natural system they are simulating, and include assumptions and generalizations in their structure and parameterization. Model predictions should therefore be interpreted taking into account the uncertainty of input parameters, of model

structure and/or of the applied numerical solution (WAGENER; GUPTA, 2005; VRUGT et al., 2008).

The assessment of agro-hydrological model prediction uncertainties is essential for water resources management for which decisions are commonly supported by model results. Uncertainty analysis provides information about the reliability of model predictions and may allow improvements toward uncertainty reduction. However, the assessment of the overall uncertainty is complex due to the inter dependence between different sources of error. The input parameters related to soil hydraulic properties have shown strong influence on agro-hydrological model predictions (VERECKEN et al., 1992), and are considered more relevant than model structure or numerical solution uncertainties (WORKMANN; SKAGGS, 1994, JOHRAR et al., 2004; BARONI et al., 2010).

Despite its importance, uncertainty analysis of agro-hydrological modelling predictions is underrepresented in literature and only a few studies have focused on the issue. To mention some reported studies, simulated actual evapotranspiration in an irrigated agricultural field in a dry region showed accurate and reliable prediction whereas deep percolation prediction was not accurate (SHAFIEI et al., 2014); rainfall spatial and temporal variation affected deep drainage predictions more than hydraulic properties in a catchment located in Australia (BENNETT et al., 2013); maize and wheat yield were sensitive to the parameters related to nutrient transport in a maize–wheat rotation cropping experiment (SUN et al., 2016); and, model structure uncertainty was assessed by simulating water balance components with different agro-hydrological models (BARONI et al., 2010; HASSANLI et al., 2016).

In addition to this implicit model uncertainty, agro-hydrological modelling becomes especially cumbersome if soil spatial variability is taken into account. Soil hydraulic properties are characterized by a strong variability in both vertical and horizontal directions even within a small field with a relatively homogeneous soil type (MITTELBACH; SENEVIRATNE, 2012; VERECKEN et al., 2016). Consequently, spatial variability of hydraulic properties should also be considered as a source of uncertainty (WALKER et al., 2003). Among agro-hydrological model applications, only a few investigated both the effect of hydraulic parameter uncertainties and spatial distribution of hydraulic properties at field scale (MAKOWSKI; WALLACH; TREMBLAY, 2002; HUPET; BOGAERT; VANCLOOSTER, 2004; LAWLESS; SEMENOV; JAMIESON, 2008; BARONI et al., 2010, BENNETT et al., 2013).

There are no well-defined guidelines to implement uncertainty analysis in a systematic and integrated manner to agro hydrological modelling (LIU; GUPTA, 2007). Many approaches based on the Generalized Likelihood Uncertainty Estimation method (GLUE; BEVEN; BINLEY, 1992) and the Monte Carlo Markov Chain method (MCMC; KUCZERA; PARENT, 1998) have been proposed to assess uncertainty in hydrological and agro-hydrological modelling over the last decades. The GLUE and MCMC have been used for both model calibration and uncertainties assessment as they are available and adaptable to nonlinear systems. The GLUE framework has been questioned in the recent literature for not being a formal Bayesian inference. The parameter and predictive distribution based on GLUE relies on subjective decisions about likelihood functions without a statistical consistency error model, which may provide questionable uncertainty boundaries with statistical incoherence (MONTOVANI; TODINI, 2006; BLASONE et al., 2008; STEDINGER et al., 2008; LI et al., 2010). The GLUE has been applied to solve problems of parameter equifinality rather than to assess model prediction uncertainties (VRUGT et al., 2008; VRUGT; TER BRAAK, 2011) whereas the MCMC method can be computationally demanding, especially when correlation among probability density functions occur, which increases the complexity and dimensionality of the sampling (LU et al., 2014).

The Latin Hypercube Sampling (LHS) is a random sampling method for Monte Carlo-based uncertainty quantification which has been widely used due to the effectiveness in generate samples preserving the probabilistic features of the variable. The advantage of this method is to cover the entire range of the variable by intervals with equal probability of occurrence with relatively small sample size (MCBAY; BECKMAN; CONOVER, 1979). The LHS is computationally cheap compared to others Monte Carlo sampling methods and can cope with many input variables (SALLABERRY; HELTON; HORA, 2007). The correlation of input variables can be incorporated in the LHS sampling scheme preserving the exact form of the marginal distributions on the input variables (IMAN; CONOVER, 1982).

In this study, we aimed to investigate the effect of soil the Mualem-van Genuchten parameters uncertainties on agro-hydrological model predictions. Using a stochastic simulation, we propose a procedure based on input parameter probability density distributions to investigate the implications of two Monte Carlo sampling methods on the model predictions. The discussion focused on simulations of crop yield and water balance components of a maize crop growing in a homogenous soil type under specific meteorological boundary conditions.

## 3.2 Material and Methods

### 3.2.1 Soil hydraulic properties

Soil hydraulic properties used in this study were obtained from a Ferralic Nitisol according to the FAO soil classification (IUSS WORKING GROUP WRB, 2015) located in Piracicaba/Brazil (X230592, Y7486483 UTM). The soil hydraulic properties from the A and Bt horizons (0.00 – 0.20 m and 0.20 – 0.40+ m, respectively) were described using the van Genuchten (1980) functions with the Mualem restriction (MUALEM, 1976):

$$\Theta = \frac{\theta - \theta_r}{\theta_s - \theta_r} = \left[ 1 + |\alpha h|^n \right]^{1-n} \quad (3.1)$$

$$K(\theta) = K_s \Theta^\lambda \left[ 1 - (1 - \Theta^{\frac{n}{n-1}})^{1-\frac{1}{n}} \right]^2 \quad (3.2)$$

where  $\Theta$  is the effective saturation;  $\theta_r$  and  $\theta_s$  are residual water content and saturated water content ( $\text{cm}^3 \text{cm}^{-3}$ ), respectively;  $h$  is matric potential (cm);  $\alpha$  ( $\text{cm}^{-1}$ ),  $n$  (-), and  $\lambda$  (-) are fitting parameters;  $K_s$  is saturated hydraulic conductivity ( $\text{cm d}^{-1}$ ).

The Mualem-van Genuchten parameters (M-VG)  $\theta_r$ ,  $\theta_s$ ,  $n$ ,  $\alpha$  and  $K_s$  were estimated by the inverse modelling option of the hydrological model HYDRUS 1-D (ŠIMŮNEK et al., 1998) employing measured water content ( $\theta_f$ ) data (Table 3.1). The water contents were obtained by Frequency Domain Reflectometry (FDR) sensors installed at 9 locations within an area of 10 x 25 m (Figure 3.1) at 0.10 and 0.30 m depths. Monitoring occurred between July and December of 2016. Data from one of the sites (Site #2) were not considered in the analysis of this study, as it appeared to refer to a compacted spot with diverging hydraulic properties.

Water content data measured between July and October were used to calibrate the M-VG parameters; the remaining period (November and December) was used to validate the results. The validation consisted in comparing simulated water contents to observed ones. The inverse modelling was evaluated using the coefficient of determination ( $r^2$ ) and Root Mean Square Error (RMSE) statistical indicators (Table 3.1). The tortuosity and connectivity parameter  $\lambda$  was not calibrated but assumed to be equal to 0.5 (MUALEM, 1976). Additional information about soil characteristics and the inverse modelling procedure can be found in chapter 2.

Figure 3.1 Schematic representation of the area with the 9 locations of FDR sensors for water content monitoring. Site number 2 (in gray) was not used in this study

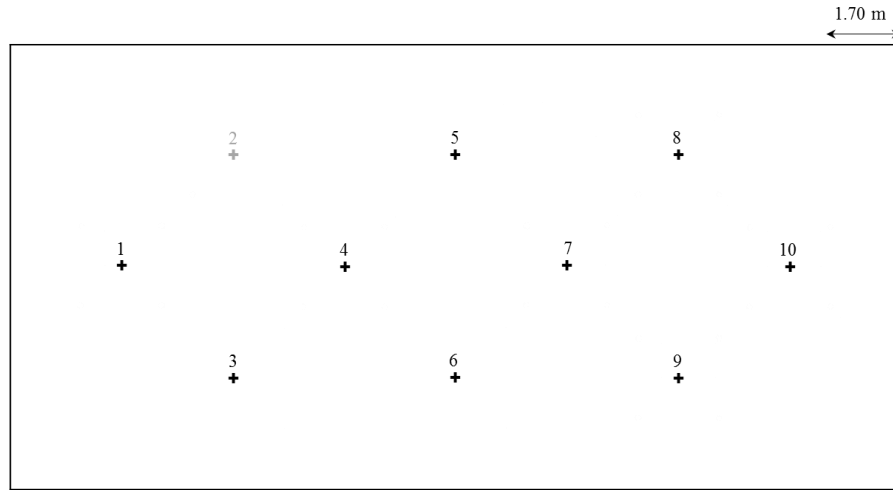


Table 3.1 Mualem-van Genuchten parameters (eq. 3.1 and eq. 3.2) and respective standard errors for A and Bt horizons obtained from inverse modelling associated with model evaluation coefficients  $r^2$  and RMSE (95% confidence interval) for all sites of the area (n = 9)

Site	Horizon	$\theta_r$	$\theta_s$	$\alpha$	$n$	$K_s$	$r^2$	RMSE
		$\text{cm}^3 \text{cm}^{-3}$	$\text{cm}^3 \text{cm}^{-3}$	$\text{cm}^{-1}$	(-)	$\text{cm d}^{-1}$		$\text{cm}^3 \text{cm}^{-3}$
1	A	$0.08 \pm 0.02$	$0.48 \pm 0.03$	$0.191 \pm 0.022$	$1.73 \pm 0.19$	$11.76 \pm 3.29$	0.96	0.01
	Bt	$0.17 \pm 0.08$	$0.44 \pm 0.02$	$0.004 \pm 0.002$	$1.31 \pm 0.15$	$13.14 \pm 6.35$		
3	A	$0.02 \pm 0.13$	$0.40 \pm 0.07$	$0.026 \pm 0.015$	$1.49 \pm 0.38$	$12.78 \pm 5.95$	0.95	0.02
	Bt	$0.10 \pm 0.36$	$0.44 \pm 0.02$	$0.007 \pm 0.005$	$1.23 \pm 0.26$	$4.16 \pm 3.59$		
4	A	$0.09 \pm 0.04$	$0.39 \pm 0.03$	$0.086 \pm 0.028$	$1.73 \pm 0.30$	$1.91 \pm 0.98$	0.89	0.02
	Bt	$0.23 \pm 0.17$	$0.45 \pm 0.07$	$0.019 \pm 0.009$	$1.37 \pm 0.62$	$30.00 \pm 21.39$		
5	A	$0.11 \pm 0.02$	$0.45 \pm 0.05$	$0.092 \pm 0.038$	$1.87 \pm 0.43$	$33.25 \pm 14.39$	0.97	0.02
	Bt	$0.20 \pm 0.17$	$0.42 \pm 0.01$	$0.015 \pm 0.008$	$1.18 \pm 0.13$	$5.71 \pm 4.21$		
6	A	$0.05 \pm 0.03$	$0.44 \pm 0.03$	$0.111 \pm 0.031$	$1.63 \pm 0.17$	$14.33 \pm 2.64$	0.92	0.02
	Bt	$0.17 \pm 0.16$	$0.40 \pm 0.06$	$0.033 \pm 0.047$	$1.30 \pm 0.33$	$10.40 \pm 35.90$		
7	A	$0.10 \pm 0.03$	$0.41 \pm 0.02$	$0.164 \pm 0.058$	$1.70 \pm 0.22$	$4.54 \pm 2.57$	0.93	0.02
	Bt	$0.25 \pm 0.28$	$0.40 \pm 0.01$	$0.023 \pm 0.035$	$1.17 \pm 0.29$	$7.33 \pm 4.17$		
8	A	$0.00 \pm 0.12$	$0.37 \pm 0.07$	$0.023 \pm 0.015$	$1.58 \pm 0.66$	$2.58 \pm 4.62$	0.93	0.03
	Bt	$0.25 \pm 0.44$	$0.40 \pm 0.05$	$0.005 \pm 0.023$	$1.28 \pm 0.6$	$7.27 \pm 24.28$		
9	A	$0.05 \pm 0.03$	$0.40 \pm 0.04$	$0.041 \pm 0.009$	$1.67 \pm 0.23$	$9.62 \pm 3.37$	0.96	0.01
	Bt	$0.09 \pm 0.16$	$0.38 \pm 0.02$	$0.011 \pm 0.007$	$1.24 \pm 0.01$	$12.90 \pm 7.53$		
10	A	$0.00 \pm 0.05$	$0.45 \pm 0.07$	$0.033 \pm 0.011$	$1.60 \pm 0.24$	$2.82 \pm 3.26$	0.92	0.03
	Bt	$0.20 \pm 0.40$	$0.47 \pm 0.07$	$0.018 \pm 0.022$	$1.26 \pm 0.56$	$24.11 \pm 32.11$		

### 3.2.2 Hydrological modelling

The SWAP model (KROES et al., 2008) was used for hydrological modelling. SWAP is a 1-D model based on an implicit numerical solution of the Richards equation allowing to simulate water, solute and heat transport in the vadose zone in interaction with crop growth. Root water uptake is accounted for by a sink term  $S$  ( $\text{cm}^3 \text{ cm}^{-3} \text{ d}^{-1}$ ), which is added to the Richards equation which reads:

$$\frac{\partial \theta}{\partial t} = \frac{\partial}{\partial z} \left[ K(\theta) \left( \frac{\partial h}{\partial z} + 1 \right) \right] - S(h) \quad (3.3)$$

where  $\theta$  is the volumetric water content ( $\text{cm}^3 \text{ cm}^{-3}$ );  $t$  is time (d);  $z$  vertical coordinate (positive upward) (cm);  $K$  is unsaturated soil hydraulic conductivity ( $\text{cm d}^{-1}$ );  $h$  is soil pressure head (cm).

The SWAP model numerically solves eq. (3.3) using the  $\theta$ - $h$ - $K$  relations described by Mualem-van Genuchten functions (eqs. 3.1 and 3.2). The top boundary condition is defined by the actual evaporation, irrigation and rainfall. Daily potential evapotranspiration is determined by Penman-Monteith equation (MONTEITH, 1965, MONTEITH, 1981) using meteorological data of air temperature, solar radiation, wind speed, and vapor pressure.

The actual plant transpiration rate ( $T_a$ ) ( $\text{cm d}^{-1}$ ) (eq. 3.4) is computed by integration of  $S$  over the root zone considering both oxygen and drought stresses according to the Feddes, Kowalik and Zaradny (1978) reduction function

$$T_a = \int_{-R_d}^0 S(h) \partial z \quad (2.4)$$

where the lower integration limit  $R_d$  is the rooting depth (cm). The actual evaporation is calculated by Darcy's equation and the bottom-boundary condition was free drainage.

### 3.2.3 Simulation scenario

The simulations were performed using the detailed crop growth module WOFOST (DE WIT et al., 2019) available in the SWAP model, simulating details about crop photosynthesis and crop development. The water balance components and crop yield were simulated for a 30 years period (1987 – 2017) for a maize crop growing every year from October 15 until March 15 under rainfed conditions. Meteorological data used in the simulations were obtained from the University of São Paulo weather station in Piracicaba, less than 1 km from the experimental area (22°42' 10" S; 47° 37' 25" W, altitude 546 m) (Figure 3.2). Table 3.2 contains the specifications of the scenario used to perform the simulations by SWAP model.

Figure 3.2 Main annual rainfall, daily solar radiation and air temperature as observed at the University of São Paulo weather station in Piracicaba/Brazil during the period 1987 – 2017

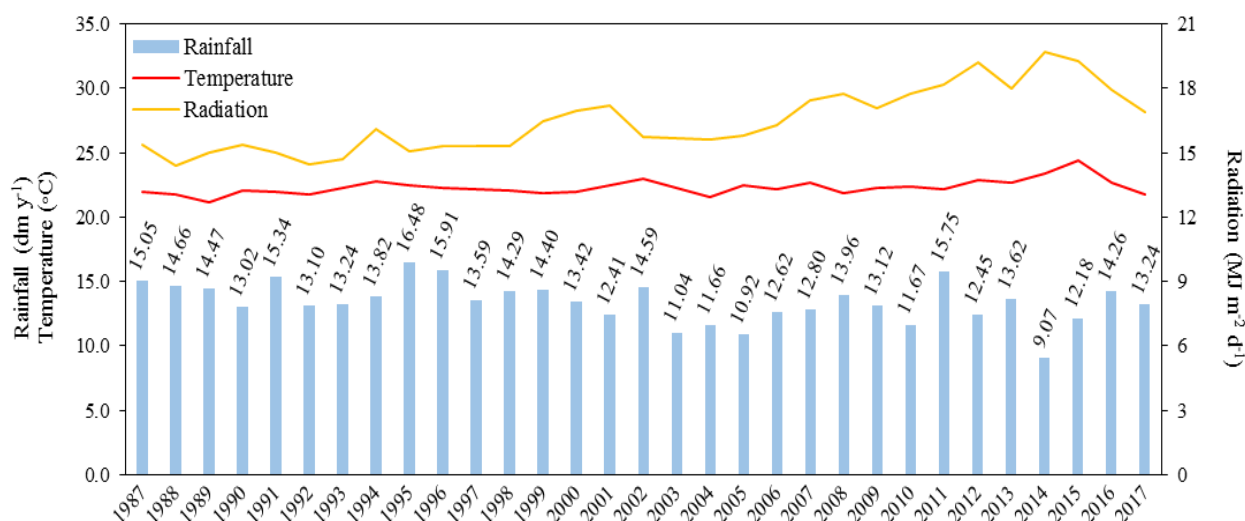


Table 3.2 Scenario specifications used to perform the SWAP simulations for maize

Section	Description	Specification	
Plant	Light extinction coefficient for diffuse visible light ( $K_{dif}$ )	0.65	
	Light extinction coefficient for direct visible light ( $K_{dir}$ )	0.75	
	Leaf area index at the beginning of simulation ( $LAI_0$ )	0.04 (m <sup>2</sup> m <sup>-2</sup> )	
	Critical pressure heads for root extraction (Feddes; Kowalik; Zaradny (1978))		$h_1 = -10$ (cm)
			$h_2 = -20$ (cm)
			$h_{3H} = -300$ (cm)
			$h_{3L} = -600$ (cm)
		$h_4 = -3000$ (cm)	
	Interception coefficient of Von Hoyningen-Hune and Braden ( $a_H$ )	0.025 (m)	
	Initial rooting depth ( $R_{di}$ )	0.05 (m)	
Maximum daily increase in rooting depth ( $R_{ri}$ )	0.022 (m)		
Maximum rooting depth crop ( $R_{dc}$ )	0.75 (m)		
Soil	Initial water content ( $\theta$ )	Pressure head as function of depth $h = -100$ (cm)	
	Vertical discretization	40 compartments of 0.01 m	
	Soil hydraulic parameters	Calibrated $\theta_s, \theta_r, \alpha, n, K_s$ (Table 3.1)	
	Bottom boundary	Fixed $\lambda = 0.5$ Free drainage	

### 3.2.4 Uncertainty analysis

Two Monte Carlo sampling methods were used analyze the influence of the Mualem-van Genuchten parameter uncertainty on the SWAP model predictions: actual crop yield ( $Y$ , kg ha<sup>-1</sup>), accumulated season runoff ( $R_{off}$ , mm), accumulated season soil evaporation ( $E_{soil}$ , mm), and accumulated season plant transpiration ( $T$ , mm). Multiple realizations of SWAP were performed using M-VG parameters obtained from random sampling and Latin Hypercube Sampling (LHS). Besides these methods, a deterministic simulation of the SWAP model using the mean of the M-VG parameters obtained from inverse modelling (Table 3.3) was performed for comparison purposes.

The first Monte Carlo sampling method aimed to analyze the influence of the M-VG parameters standard errors obtained from the inverse modelling on the SWAP predictions. Random samples of each M-VG parameter were drawn from normal distribution and respective standard errors (Table 3.1), supposing independence between the parameters. This method will be referred as MCRS.

To avoid excessive simulations and optimize processing time, the samples size,  $N$ , of each M-VG parameter was determined by a variance analysis. The sample size was considered adequate when the parameter variance became less than  $10^{-3}$ , corresponding to  $N = 500$ . Therefore, 500 random values were generated using the mean and respective standard error of each hydraulic parameter. Some M-VG parameter combinations are less likely to occur in reality, and the model may fail to converge, especially for values that are at the tails of the normal distribution. To avoid this, the upper and lower 5% of the distribution tails were excluded. Due to the relatively high standard errors, negative values of  $\alpha$  and  $K_s$ , as well as  $n$ -values  $\leq 1$  were sometimes generated but considered as non-feasible values and eliminated. For this sampling method, 270 M-VG parameter sets per site were eliminated and the remaining 230 ( $9 \times 230 = 2070$  in total) were used to perform simulations with the SWAP model.

The second sampling method used the Monte Carlo Latin Hypercube Sampling and will be referred as MCLHS. The MCLHS is a type of stratified Monte Carlo sampling (MCKAY; BECKMAN; CONOVER, 1979), which provide non-collapsing and more space-filling results compared to simple random sampling techniques (FANG; MA; WINKER, 2000, HELTON; DAVIS; JOHNSON, 2015). The LHS is a generalization of the Latin Square sampling scheme whereby only one sample is taken from each row and column of a square grid where the input variables have all portions of its range represented during the sampling procedure.

To generate a sample of size  $m$  from the  $n$  variables with the distributions  $D_1, D_2, \dots, D_n$ , the range  $X_j$  of each variable  $x_j$  is divided into  $m$  non-overlapping contiguous intervals

$$X_{ij}, i = 1, 2, \dots, m$$

of equal probability ( $1/N$ ) in consistency with the corresponding  $D_j$  distribution. One random value of the variable  $x_j$  is selected from the interval  $X_{ij}$  in consistency with the distribution  $D_j$  for  $i = 1, 2, \dots, m$  and  $j = 1, 2, \dots, n$ . After, the  $m$  values for  $x_1$  are randomly combined without replacement with the  $m$  values for  $x_2$  to produce the ordered pairs

$$[x_{i1}, x_{i2}], i = 1, 2, \dots, m.$$

Randomly, the previous pairs are combined without replacement with the  $m$  values for  $x_3$  producing the ordered triples

$$[x_{i1}, x_{i2}, x_{i3}], i = 1, 2, \dots, m.$$

The sampling process is complete for all  $n$  variables, resulting in a LHS of size  $m$  from  $n$  variables ( $x$ )

$$x_i = [x_{i1}, x_{i2}, x_{in}], i = 1, 2, \dots, m \text{ (SALLABERRY; HELTON; HORA, 2007)}.$$

The Pearson correlation between the M-VG parameters from each horizon and between horizons were included in the sample generation using the LHScorr function of the lhs R

package (R CORE TEAM, 2018). This function force the correlation matrix to a predictive value using the Huntington-Lyrintzis algorithm preserving the exact form of the marginal distributions on the input variables (IMAN; CONOVER, 1982). (HUNTINGTON; LYRINTZIS, 1998). For this method, 1000 values of each M-VG parameter were used to perform the simulations with SWAP

### 3.2.5 Modelling validation

Soil water content over time and depth is a primary output value of the SWAP model and can be used to interpret the validity of modelling results. Obtained values of water content predicted by the SWAP model using the M-VG parameters from the MCRS and MCLHS sampling methods were compared with the measured values ( $\theta_f$ ) obtained from the field experiment between October, 15 and December, 31 2016.

## 3.3 Results and Discussion

### 3.3.1 Hydraulic parameters uncertainty

The probability density distributions of the Mualem-van Genuchten parameters obtained using the two sampling methods, MCRS and MCLHS, are shown in Figure 3.3. The probability density functions represented the uncertainty of each soil hydraulic parameter that was used as input data for the SWAP model. The statistical characteristics of the soil hydraulic parameter are shown in Table 3.3.

The ranges of the hydraulic parameters distributions from MCRS were wider compared to MCLHS (Figure 3.3) duo to the fact that the relatively high standard errors used in MCRS resulted in wider ranges of sampled values. Meanwhile, the ranges from MCLHS were smaller since the LHS takes samples within the interval provided by the generated cumulative distribution (MCBAY; BECKMAN; CONOVER, 1979). The width differences were especially relevant for parameter  $\theta_r$ ,  $\theta_s$  and  $n$  for both horizons. For MCRS, the  $n$ -values were distributed over the x-axis with low density for both horizons, whereas for MCLHS, the ranges were narrow with high density.

Both MCRS and MCLHS provided similar distribution of  $\alpha$  and  $K_s$  parameters. Although the ranges were distinct between the methods, the high densities regions were relatively similar with low density in the tails. The shapes of the probability density

distributions also were distinct for both horizons. MCLHS presented multiple modal distribution with multiple regions with high densities, whereas for MCRS the distributions were mostly unimodal, or multimodal with smoothed peaks (Figure 3.3).

For MCRS, the presence of heavy tails in the probability density distributions provided a displaced mean from the high-density regions for  $n$  and  $K_s$  (Figure 3.4), whereas the presence of light tails for the  $\theta_r$  and  $\theta_s$ , promoted means closer to these regions. The presence of multi modes of multimodal distributions or the presence of heavy tails in unimodal distributions demonstrates the concern of using the mean as indicator of central tendency as representative of the stochastic distribution. Moreover, the mean is commonly used as the representative value of soil hydraulic properties (e.g, M-VG parameters) for a certain soil type, which may provide erroneous interpretation of soil transport phenomena.

Figure 3.5 illustrates extreme scenarios of water retention curves using the minimum and maximum values of the M-VG parameters obtained from MCRS and MCLHS. These values were selected only for one M-VG parameters from a certain set whereas the others remained with their original values. The MCRS provided more heterogeneous WRC shapes compared to MCLHS, as expected as the ranges of the hydraulic parameters from this method were wider (Table 3.3). The minimum  $\alpha$  and  $n$ -values obtained from MCRS generated flatter WRCs which impair the soil to desaturate whereas higher values of  $n$  generated steep WRCs allowing water release in the low suction range (OR; TULLER, 1999, WANG et al., 2017).

Figure 3.3 Probability density distributions of the Mualem-van Genuchten parameters obtained from Monte Carlo Random Sampling (MCRS) ( $n = 1256$ ) and Monte Carlo Latin Hypercube Sampling (MCLHS) ( $n = 1000$ ). Dashed lines refers to the mean values for MCRS and MCLHS. Mean lines of  $\theta_s$  from Bt horizon are overlapped

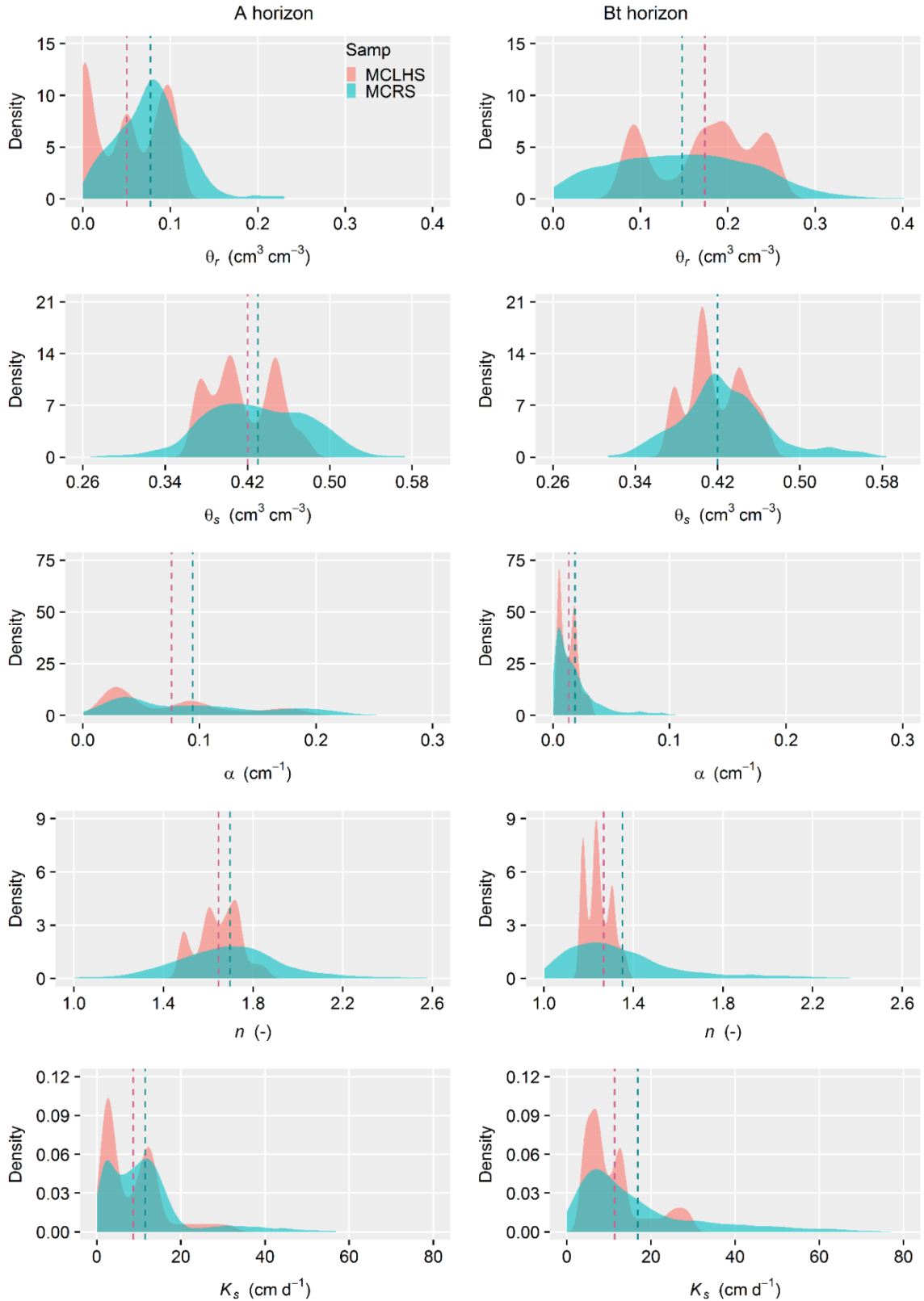


Figure 3.4 Quantile–quantile plots depicting heavy tails from  $n$  and  $K_s$  probability distributions functions of the Bt horizon based on Monte Carlo Random Sampling (MCRS)

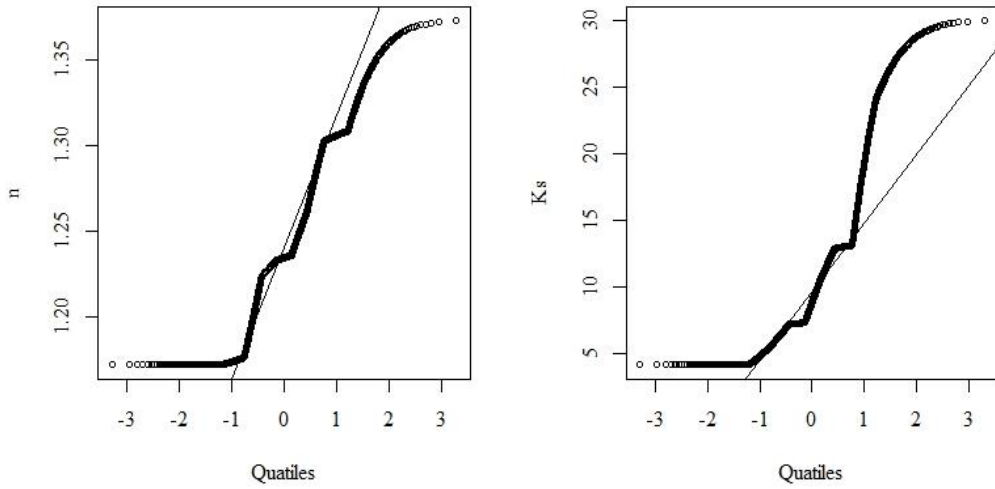


Figure 3.5 Water retention curves using maximum and minimum values of the Mualem-van Genuchten parameters for Monte Carlo Random Sampling (MCRS) and Monte Carlo Latin Hypercube Sampling (MCLHS) for A and Bt horizons. Thick lines represents the curves using the mean values

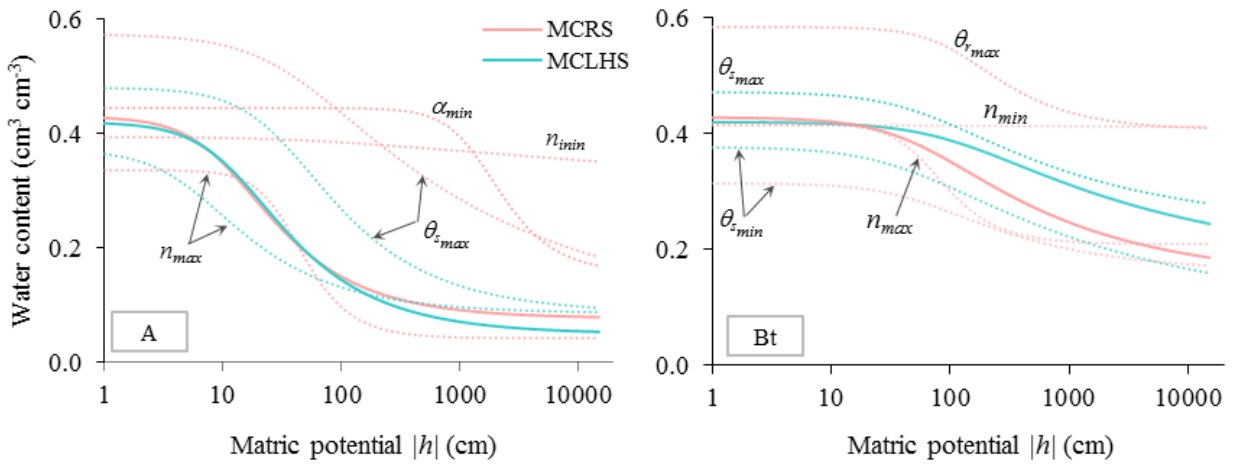


Table 3.3 Statistical characteristics of the Mualem-van Genuchten parameters for Random Sampling (MCRS) (n = 1256) and Monte Carlo Latin Hypercube Sampling (MCLHS) (n = 1000) for A and Bt horizons

Method	Statistics	Horizon	$\theta_r$	$\theta_s$	$\alpha$	$n$	$K_s$
			cm <sup>3</sup> cm <sup>-3</sup>		cm <sup>-1</sup>	(-)	cm d <sup>-1</sup>
MCRS	Mean	A	0.08	0.43	0.102	1.71	12.46
		Bt	0.15	0.42	0.019	1.33	14.93
	Min	A	0.00	0.28	0.004	1.00	0.11
		Bt	0.00	0.31	0.000	1.00	0.03
	Max	A	0.23	0.54	0.256	2.58	56.83
		Bt	0.37	0.57	0.105	2.37	68.70
	SD	A	0.04	0.05	0.062	0.24	10.19
		Bt	0.08	0.04	0.020	0.24	13.20
MCLHS	Mean	A	0.05	0.42	0.076	1.65	8.66
		Bt	0.17	0.42	0.013	1.24	11.34
	Min	A	0.00	0.37	0.023	1.49	1.95
		Bt	0.09	0.38	0.004	1.17	4.16
	Max	A	0.11	0.48	0.191	1.87	33.16
		Bt	0.25	0.47	0.033	1.37	29.98
	SD	A	0.04	0.03	0.052	0.10	7.09
		Bt	0.06	0.03	0.008	0.06	7.12

### 3.3.2 Uncertainty of modelling results

Simulated actual crop yield ( $Y$ ), accumulated season runoff ( $R_{off}$ ), accumulated season plant transpiration ( $T$ ), accumulated season soil evaporation ( $E_{soil}$ ), accumulated season bottom flux ( $q_{bot}$ ), and their statistics obtained from stochastic realizations performed with SWAP using MCRS and MCLHS sampling methods for 30 growing seasons are shown in Figure 3.6 and Table 3.4. Some combinations of hydraulic parameters, especially those in which the difference between  $\theta_s$  and  $\theta_r$  was small, caused numerical issues in the SWAP model. Therefore, a minimum of 0.15 was adopted for this difference, reducing the number of simulations of MCRS from 2070 to 1256. For MCLHS, this problem was not detected, i.e., differences between  $\theta_s$  and  $\theta_r$  were large enough in all cases.

The mean values of simulated  $Y$  and  $T$  were similar for MCRS and MCLHS, however for MCRS low values of land productivity and plant transpiration were obtained due the presence of heavy tails in their probability density distribution (Figure 3.6 and Table 3.4) The wide range of M-VG parameters obtained by MCRS (Table 3.3) generated unrealistic hydraulic parameter combinations for this soil type which simulated extremely low values of  $Y$  and  $T$  (minimum of 11.87 kg ha<sup>-1</sup> and 43.12 mm, respectively). On the other hand, the narrower range of M-VG parameters obtained from MCLHS generated narrower range and more realistic values of land productivity and plant transpiration. Although the mean values of  $Y$  were below the Brazilian mean land productivity (4.900 kg ha<sup>-1</sup>, CONAB, 2016),

the  $T$  values for both sampling methods were similar for those found by Pinheiro; De Jong van Lier; Šimůnek. (2019) for the similar climatic conditions and soil type.

The mean values of  $E_{soil}$  were similar between the sampling methods, but again the presence of heavy tails in the probability density distribution obtained using MCRS generated high values of soil evaporation. This may promoted high water loss in the soil surface reducing crop available water and possibly causing drought stresses affecting land productivity. Considering the evaporation rate at the soil surface function of soil hydraulic properties, climatic conditions and land cover, and assuming only hydraulic properties changings in thus study, the hydraulic parameters related to  $K$  determination (eq. 3.2), e.g.,  $n$  and  $K_s$ , may promoted  $E_{soil}$  differences between sampling methods.

Soil hydraulic properties, especially hydraulic conductivity mostly affect runoff and bottom flux. The low values of  $K_s$  in the A horizon (Table 3.1) promoted slow infiltration of water into the soil during intense rainfall events reducing available water to plants. While some high values of  $K_s$  from the Bt horizon associated with macropores present in the subsurface layer enhanced release of water in the bottom of the soil profile. Besides the influence of  $K_s$ , the adoption of the pore connectivity value ( $\lambda$ ) of 0.5 from Mualem (1976) likely to negatively affected the  $K$  determination introducing more uncertainty in  $R_{off}$ ,  $E_{soil}$  and  $q_{bot}$  predictions (VERECKEN et al., 2010, DE JONG VAN LIER; WENDROTH., 2016). The high uncertainty associated to the  $K_s$  obtained by the inverse modelling (Table 3.1) may enhanced the uncertainty of soil hydrological related-processes simulation, evidencing the importance of proper soil hydraulic properties determination, as well as the difficult of obtain soil hydraulic properties from transient water flow in field conditions by inverse modelling.

The probability density distributions shape of  $E_{soil}$  were distinct for MCRS and MCLHS, whilst the shape of MCRS tended to be unimodal, the MCLHS presented multimodal distribution with three peaks with high probability of occurrence. The  $R_{off}$  and  $q_{bot}$  showed bimodal probability density distributions for both sampling methods. Wherein one peak of the distribution matched for MCRS and MCLHS, the other was more pronounced for MCLHS. For this type of distribution, the mean are displaced from the high density regions. Although some distributions obtained by MCRS and MCLHS tented unimodal distribution, none of the SWAP predictions were normally distributed according to the Shapiro-Wilk test (95% confidence level).

The deterministic simulation of the SWAP model using the mean values of M-VG parameters (Table 3.1) is also shown in Figure 3.6. The simulated  $Y$  and  $T$  were close to the high density regions for both sampling methods, whereas for  $E_{soil}$ , the deterministic approach matched high density region only of MCRS. Simulated  $R_{off}$  and  $q_{bot}$  were close to high density regions of one peak of the bimodal distribution. Although the deterministic approach may indicate some tendency in the simulated  $Y$ ,  $T$  and  $E_{soil}$ , no conclusions about their frequency can be drawn. Moreover, for  $R_{off}$  and  $q_{bot}$ , the deterministic standpoint is withholding information about the bimodal distribution.

With these results we aimed to demonstrate the dependence of the simulated results performed by SWAP model to the sampling method. The uncertainty analysis is a key tool for more reliable interpretation of the water balance and crop yield in agro-hydrological systems and should be considered in agro-modelling studies.

Figure 3.6 Probability density function of the SWAP results, actual crop yield ( $Y$ ), accumulated season runoff ( $R_{off}$ ), accumulated season plant transpiration ( $T$ ), accumulated season soil evaporation ( $E_{soil}$ ), and accumulated season bottom flux ( $q_{bot}$ ) obtained using Monte Carlo Random Sampling (MCRS) ( $n = 1256$ ) and Monte Carlo Latin Hypercube Sampling (MCLHS) ( $n = 1000$ ). Dashed lines refers to the mean values for each sampling method and the black line refers to deterministic simulation ( $n = 9$ )

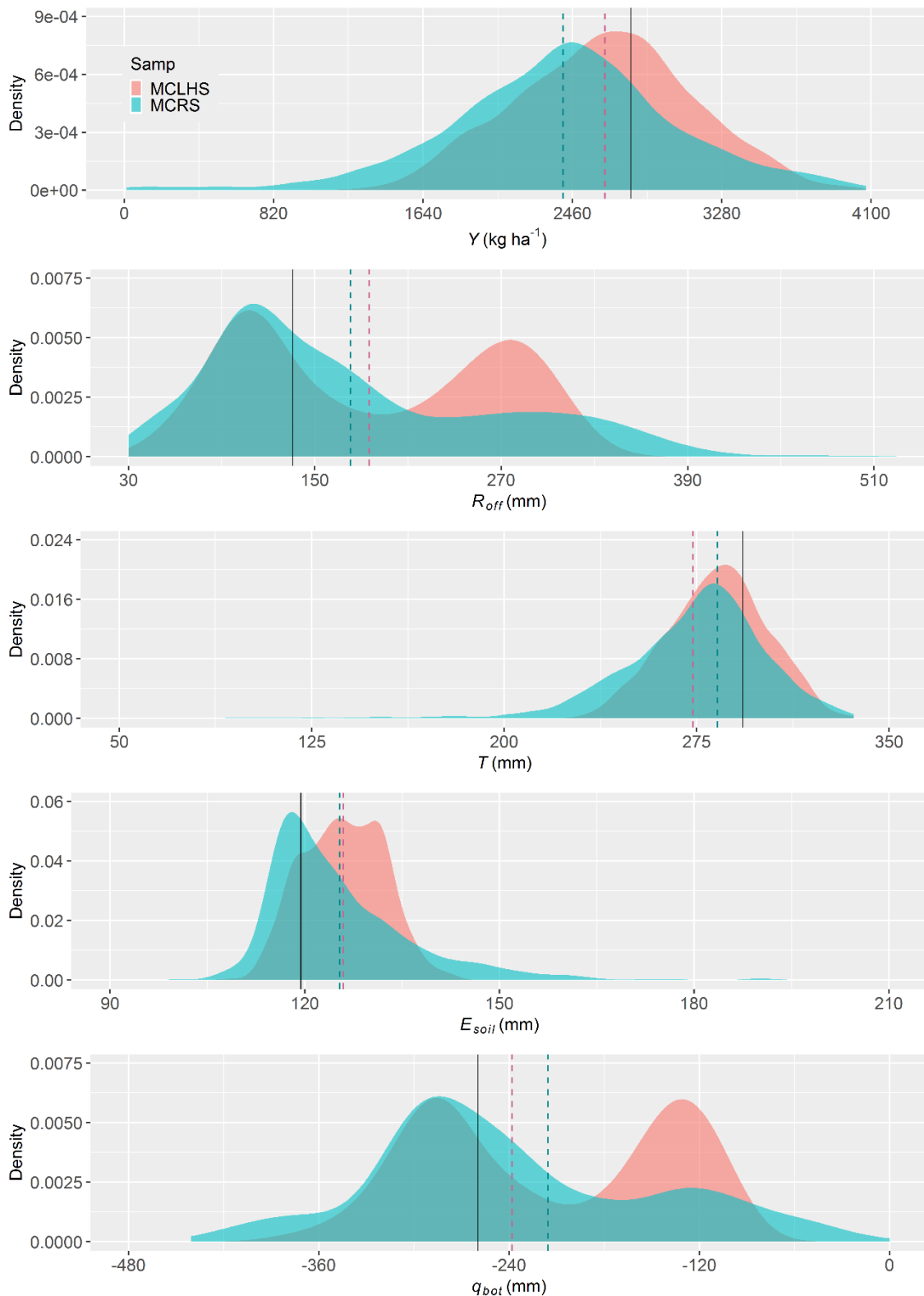


Table 3.4 Statistical characteristics of water balance components and crop yield for Monte Carlo Random Sampling (MCRS) and Monte Carlo Latin Hypercube Sampling (MCLHS). Values for runoff, plant transpiration, soil evaporation and bottom flux are cumulative

Method	Realizations	Statistics	Actual crop yield ( $Y$ )	Runoff ( $R_{off}$ )	Plant transpiration ( $T$ )	Soil evaporation ( $E_{soil}$ )	Bottom flux ( $q_{bot}$ )
			kg ha <sup>-1</sup>	mm (season)			
MCRS	1256	Mean	2409.52	172.84	273.48	125.38	-238.21
		Min	11.87	30.13	43.12	99.06	-440.39
		Max	4071.32	525.43	336.26	198.80	-0.09
		SD	631.08	90.92	29.63	11.48	88.57
MCLHS	1000	Mean	2638.43	184.91	283.03	125.95	-215.42
		Min	1266.46	40.82	228.91	107.77	-388.03
		Max	4017.00	341.90	334.22	143.33	-85.36
		SD	481.44	82.54	19.12	6.22	79.04

### 3.3.3 Simulated water contents

Water contents from the field measuring were compared with simulated water contents predict by the SWAP model. The 50% percentile of simulated water contents ( $\theta_{50\%}$ ) and the mean of the ten lower ( $L_{W10}$ ) and upper ( $U_{p10}$ ) M-VG parameters were used as central and lower and upper boundaries, respectively.

The model well described  $\theta_{50\%}$  with relatively high accuracy for both horizons (Figure 3.7a), however misestimates occurred frequently. In the A horizon,  $\theta_{50\%}$  was underestimated most of the period except after high intensity rainfall events and for the longest rainless period (18 to 27 November), in which water contents were overestimated. In general,  $\theta_{50\%}$  was underestimated with the  $\theta_f$  increment (higher than  $0.25 \text{ cm}^3 \text{ cm}^{-3}$ ) for both sampling methods (Figure 3.7b). In the Bt horizon,  $\theta_{50\%}$  was underestimated during the entire simulated period, however it followed the  $\theta_f$  trend better than for the A horizon (Figure 3.7b).

The difference between  $\theta_{50\%}$  and  $\theta_f$  may be caused due to measuring errors in the field and model limitations. In the field, measurements of water content are prone to many factors which can lead to erroneous results. First, issues regarding FDR technique capability to determine soil water content should be considered (SUSHA; SINGH; BAGHINI, 2014). Second, issues regarding the probe installation can affect the measurements. Air gaps between the soil and the probe is a common concern regarding this technique (RAO; SINGH, 2011), moreover the presence of macropores and the roughness of the soil surface may affect water flow near the measurement site causing differences between measured and simulated water contents. The depth of water content determination in the field is also another drawback because it may slight differ from the adopted depth in the simulation.

Besides the issues with the observed field values, the SWAP model has its own limitations which affect predicted water contents. Although the SWAP model uses physical soil process descriptions, there are limitations to describe complex processes, e.g., soil evaporation (OR et al., 2013), which affect the water balance simulation. Also hysteresis in retention and conductivity properties may be an important limitation in field studies where water contents increase and decrease over time. Hysteretic behavior was not included in the analysis and simulations performed in this study.

Simulated soil water contents from MCRS showed a wider range compared to MCLHS for both horizons, especially for the Bt. The lower ( $Lw_{10}$ ) and upper ( $Up_{10}$ ) bounds were mostly determined by the  $\theta_s$  and  $n$  parameters for both horizons (Table 3.5). The  $Up_{10}$  of MCRS present higher values of  $\theta_s$  and lower  $n$  values, whereas for the  $Lw_{10}$ , higher values of  $n$  mostly contributed to lower  $\theta_{50\%}$  since  $\theta_s$  values were similar for both sampling methods.

Figure 3.7 (a) Measured and simulated water contents with the lower limit (0.05 percentile) and upper limit (0.95 percentile) performed by the SWAP model for Monte Carlo Random Sampling (MCRS) ( $n = 1256$ ) and Monte Carlo Latin Hypercube Sampling (MCLHS) ( $n = 1000$ ) for A and Bt horizons. (b) Mean  $\theta_f$  from all sites of the area ( $n = 9$ ) and  $\theta_{50\%}$  for MCRS and MCLHS for A and Bt horizons

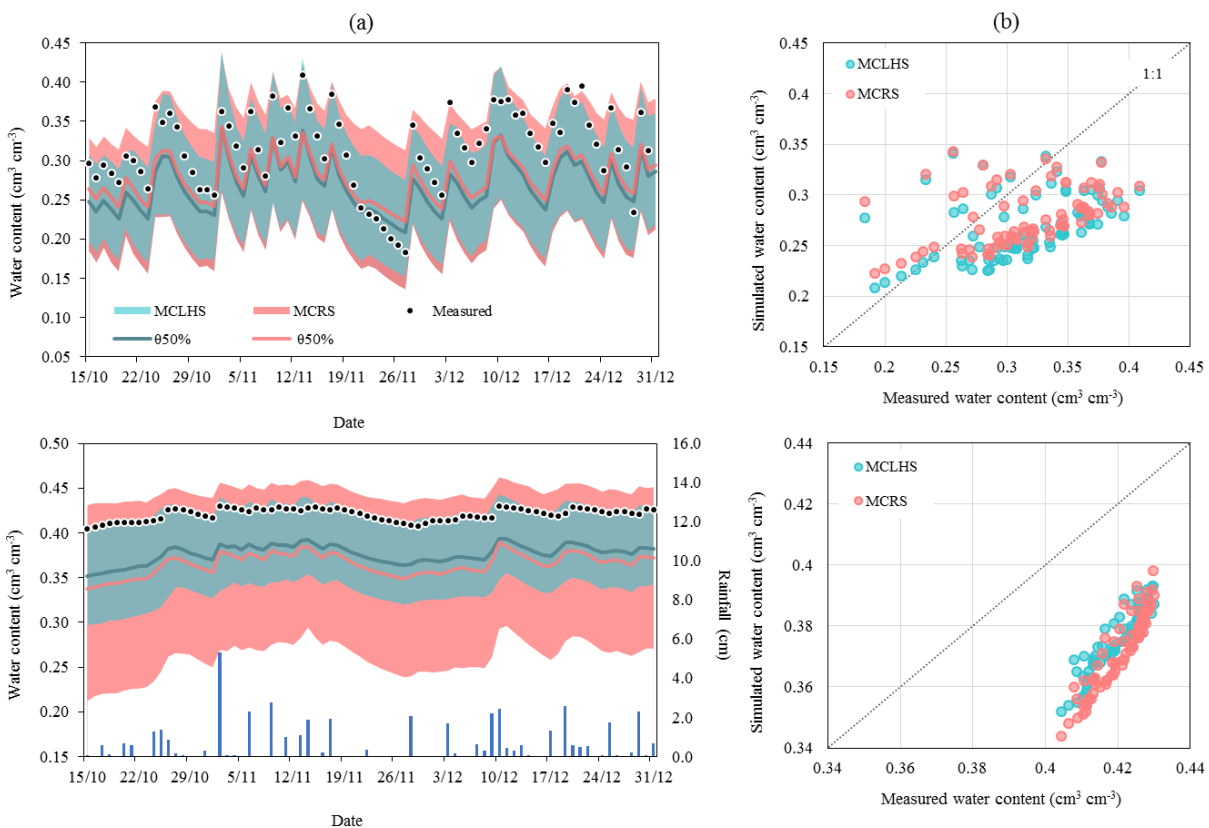


Table 3.5 Mean of the ten lower ( $L_{w10}$ ) and upper ( $U_{p10}$ ) Mualem-van Genuchten parameters for Monte Carlo Random Sampling (MCRS) and Monte Carlo Latin Hypercube Sampling (MCLHS) for A and Bt horizons

Method	Bound	Horizon	$\theta_r$	$\theta_s$	$\alpha$	$n$	$K_s$
			cm <sup>3</sup> cm <sup>-3</sup>	cm <sup>3</sup> cm <sup>-3</sup>	cm <sup>-1</sup>	-	cm d <sup>-1</sup>
MCRS	$L_{w10}$	A	0.04	0.35	0.040	2.18	15.97
		Bt	0.03	0.37	0.023	1.86	38.40
	$U_{p10}$	A	0.02	0.50	0.090	1.29	7.22
		Bt	0.01	0.51	0.282	1.14	20.22
MCLHS	$L_{w10}$	A	0.03	0.35	0.083	1.61	17.01
		Bt	0.02	0.38	0.101	1.29	20.43
	$U_{p10}$	A	0.05	0.46	0.091	1.60	3.06
		Bt	0.01	0.47	0.217	1.21	5.34

### 3.4 Conclusions

Uncertainty analysis of SWAP model predictions for a 30 years simulation period for a soil under rainfed maize crop was realized using two Monte Carlo sampling methods. MCRS and MCLHS generated distinct ranges and formats of the probability density distributions of the Mualem-van Genuchten parameters, especially for  $n$ , whereas  $\alpha$  did not showed much differences.

The simulated water balance and crop yield also showed distinct ranges and shapes of probability density distributions for MCRS and MCLHS. The MCRS generated wider range of simulated results, while for  $R_{off}$ ,  $E_{soil}$  and  $q_{bot}$  showed remarkable differences in the probability density distributions shape. The relatively high standard error of M-VG parameters from MCRS may enhanced the uncertainty of the simulated results since it generated wider ranges of hydraulic parameters and because several restriction were imposed to eliminate unrealistic combinations of hydraulic parameters. In this study, we strongly recommend the LHS technique for the stochastic procedure since it seemed to generate more reliable hydraulic parameter combinations.

The stochastic realizations may provide useful information about the uncertainties of model SWAP predictions and should be preferred over a mere deterministic method, which often provides results diverging those obtained from probabilistic methods. Moreover, uncertainty analysis provides key informations for risk analysis.

### References

BARONI, G.; FACCHI, A.; GANDOLFI, C.; ORTUANI, B.; HORESCHI, D.; VAN DAM, J.C. Uncertainty in the determination of soil hydraulic parameters and its influence on the performance of two hydrological models of different complexity. **Hydrological and Earth System Sciences**, Gottingen, v. 14, p. 251–270, 2010.

BENNETT, S.J.; THOMAS, F.A.; BISHOP, R.; VERVOORT, W. Using SWAP to quantify space and time related uncertainty in deep drainage model estimates: A case study from northern NSW, Australia. **Agricultural Water Management**, Amsterdam, v. 130, p. 142-153, 2013.

BEVEN, K.; BINLEY, A. The future of distributed models: Model calibration and uncertainty prediction. **Hydrological Processes**, Chichester, v. 6, n. 3, p. 279-298, 1992.

BLACK, T.A.; GARDNER, W.R.; THURTELL, G.W. The prediction of evaporation, drainage, and soil water storage for a bare soil. **Science Society American Journal**, Madison, v. 33, p. 655- 660, 1969.

BLASONE, R.-S.; VRUGT, J.A.; MADSEN, H.; ROSBJERG, D.; ROBINSON, B.A.; ZYVOLOSKI, G.A. Generalized likelihood uncertainty estimation (GLUE) using adaptive Markov chain Monte Carlo sampling. **Advances in Water Resources**, Kidlington, v. 31, n. 4, p. 630-648, 2008.

BOESTEN, J.J.T.I.; STROOSNIJDER, L. Simple model for daily evaporation from fallow tilled soil under spring conditions in a temperate climate. **Netherlands Journal of Agricultural Science**, Wageningen, v. 34, p. 75-90, 1986.

COMPANHIA NACIONAL DE ABASTECIMENTO – CONAB. **Informações agropecuárias - 2016**. Brasília, DF, 2019. Available at: <https://www.conab.gov.br/info-agro>. Accessed on: 20/04/219.

DE JONG VAN LIER, Q.; VAN DAM, J.C.; METSELAAR, K.; DE JONG, R.; DUIJNISVELD, W.H.M. Macroscopic root water uptake distributions using matric flux potential approach. **Vadose Zone Journal**, Madison, v. 7, n. 3, p. 1065-1078, 2008.

DE JONG VAN LIER, Q.; WENDROTH, O. Reexamination of the field capacity concept in a Brazilian Oxisol. **Soil Science Society of American Journal**, Madison, v. 79, p. 9–19. 2016.

DE WIT, A.; BOOGAARD, H.; FUMAGALLI, D.; JANSSEN, S.; KNAPEN, R.; VAN KRAALINGEN, D.; SUPIT, I.; VAN DER WIJNGAART, R.; VAN DIEPEN, K. 25 years of the WOFOST cropping systems model. **Agricultural Systems**, Amsterdam, v. 168, p. 154-167, 2019.

FACCHI, A.; ORTUANI, B.; MAGGI, D.; GANDOLFI, C. Coupled SVAT-groundwater model for water resources simulation in irrigated alluvial plains. **Environmental Modelling Software**, Amsterdam, v. 19, n. 11, p. 1053-1063, 2004.

FANG, K.-T.; MA C.-X.; WINKER, P. Centered L2-discrepancy of random sampling and Latin hypercube design, and construction of uniform designs. **Mathematics of Computation**, Rhode Island, v. 71, n. 237, p. 275–296, 2000.

FEDDES, R.A.; KOWALIK, P.J.; ZARADNY, H. **Simulation of field use and crop yield**. Wageningen, NE: Centre for Agricultural Publishing and Documentation, 1978. 189 p.

HASSANLI, M.; EBRAHIMIAN, H.; MOHAMMADI, E.; RAHIMI, A.; SHOKOUHI, A. Simulating maize yields when irrigating with saline water, using the AquaCrop, SALTMED, and SWAP models. **Agricultural Water Management**, Amsterdam, v. 176, p. 91-99, 2016.

HE, J.; DUKES, M.; JONES, J.; GRAHAM, W.D.; JUDGE, J. Applying GLUE for estimating CERES-maize genetic and soil parameters for sweet corn production. **Transactions of the ASABE**, Saint Joseph, v. 52, n. 6, p. 1907–1921, 2009.

HELTON, J.C.; DAVIS, F.J.; JOHNSON, J.D. A comparison of uncertainty and sensitivity analysis results obtained with random and Latin hypercube sampling. **Reliability Engineering & Systems Safety**, Amsterdam, v. 89, n. 3, p. 305–330, 2005.

HUPET, F.; BOGAERT, P.; VANCLOOSTER, M. Quantifying the localscale uncertainty of estimated actual evapotranspiration. **Hydrological Processes**, Chichester, v. 18, n. 17, p. 3415–3434, 2004.

HUNTINGTON, D.E.; LYRINTZIS, C.S. Improvements to and limitations of Latin hypercube sampling. **Probabilistic Engineering Mechanics**, Amsterdam, v. 13, n. 4, p. 245-253, 1998.

IMAN, R.L.; CONOVER, W.J. A distribution-free approach to inducing rank correlation among input variables. **Communications in Statistics: Simulation and Computation B**, London, v.11, n. 3, p. 311–34, 1982.

IUSS WORKING GROUP WRB. **World reference base for soil resources 2014: International soil classification system for naming soils and creating legends for soil maps**. Rome: FAO, 2015. 203 p. (World Soil Resources Reports, 106).

JOHRAR, R.K.; VAN DAM, J.C.; BASTIAANSAN, W.G.M.; FEDDES, R.A.: Calibration of effective soil hydraulic parameters of heterogeneous soil profiles. **Journal of Hydrology**, Amsterdam, v. 285, n. 1-4, p. 233–247, 2004.

KROES, J.G.; VAN DAM, J.C.; GROENENDIJK, P.; HENDRIKS, R.F.A.; JACOBS, C.M.J. **SWAP version 3.2: Theory description and user manual**. Wageningen: Alterra 2008. 262 p. (Alterra Report, 1649).

KUCZERA, G.; PARENT, E., Monte Carlo assessment of parameter uncertainty in conceptual catchment models: the Metropolis algorithm. **Journal of Hydrology**, Amsterdam, v. 211, n. 1–4, p. 69–85, 1998.

LAWLESS, C.; SEMENOV, M.A.; JAMIESON, P.D. Quantifying the effect of uncertainty in soil moisture characteristics on plant growth using a crop simulation model. **Field Crops Research**, Amsterdam, v. 106, n. 2, p. 138–147, 2008.

LI, L.; JUN, X.; CHONG-YU, X.; SINGH, V.P. Evaluation of the subjective factors of the GLUE method and comparison with the formal Bayesian method in uncertainty assessment of hydrological models. **Journal of Hydrology**, Amsterdam, v. 390, n. 3-4, p. 210–221, 2010.

LIU, Y.; GUPTA, H.V. Uncertainty in hydrologic modeling: Toward an integrated data assimilation framework. **Water Resources Research**, Washington, v. 43, n. 7, 2007. doi:10.1029/2006WR005756.

LU, D.; YE, M, HILL, M.C.; POETER, E.P.; CURTIS, G.P. A computer program for uncertainty analysis integrating regression and Bayesian methods. **Environmental Modelling & Software**, Amsterdam, v. 60, p. 45-56, 2014.

MCKAY, M.D.; BECKMAN, R.J.; CONOVER, W.J. A comparison of three methods for selecting values of input variables in the analysis of output from a computer code. **Technometrics**, London, v. 21, n. 2, p. 239–245, 1979.

MAKOWSKI, D.; WALLACH, D.; TREMBLAY, M. Using a Bayesian approach to parameter estimation; comparison of the GLUE and MCMC methods. **Agronomie**, Paris, v. 22, p. 191-203, 2002.

MAAS, E.V.; HOFFMAN, G.J. Crop salt tolerance-current assessment. **Journal of Irrigation and Drainage**, Reston, v. 103, n. 2, p. 115-134, 1977.

MANTOVANI, P.; TODINI, E. Hydrological forecasting uncertainty assessment: incoherence of the GLUE methodology. **Journal of Hydrology**, Amsterdam, v. 330, n. 1-2, p. 368–381, 2006.

MITTELBACH, H.; SENEVIRATNE, S.I. A new perspective on the spatio-temporal variability of soil moisture: temporal dynamics versus time-invariant contributions. **Hydrological and Earth System Sciences**, Gottingen, v. 16, p. 2169–2179, 2012.

MUALEM, Y. A new model for predicting the hydraulic conductivity of unsaturated porous media. **Water Resources Research**, Washington, v. 12, n. 3, p. 513-522, 1976.

MONTEITH, J.L. Evaporation and environment. In: FOGG G.E. (Ed.). **The state and movement of water in living organisms**. Cambridge: Cambridge University Press, 1965. p. 205-234.

MONTEITH, J.L. Evaporation and surface temperature. **Quarterly Journal of the Royal Meteorological Society**, Chichester, v. 107, p. 1-27, 1981.

PINHEIRO, E.A.R.; DE JONG VAN LIER, Q.; ŠIMŮNEK, J. The role of soil hydraulic properties in crop water use efficiency: A process-based analysis for some Brazilian scenarios. **Agricultural Systems**, Amsterdam, v. 173, p. 364-377, 2019.

OR, D.; LEHMANN, P.; SHAHRAEENI, E.; SHOKRI, N. Advances in soil evaporation physics-A review. **Vadose Zone Journal**, Madison, v. 12, n. 4, p. 1-16, 2013.

OR, D.; TULLER, M. Liquid retention and interfacial area in variably saturated porous media: Upscaling from single-pore to sample scale model. **Water Resources Research**, Washington, v. 35, n. 12, p. 3591–3605, 1999.

R CORE TEAM. **R. A language and environment for statistics computing**. Vienna: R Foundation for Statistical Computing, 2018

RAO, B.H.; SINGH, D.N. Moisture content determination by TDR and capacitance techniques: a comparative study. **International Journal of Earth Sciences and Engineering**, Hyderabad, v. 4, n. 6, 2011.

SALLABERRY, C.J.; HELTON, J.C.; HORA, S.C. Extension of Latin Hypercube Samples with correlated variables. **Reliability Engineering and System Safety**, Amsterdam, v. 93, p. 1047–1059, 2008.

SHAFIEI, M.; GHAHRAMAN, B.; SAGHAFIAN, B.; DAVARY, K.; PANDE, S.; VAZIFEDOUST, M. Uncertainty assessment of the agro-hydrological SWAP model application at field scale: A case study in a dry region. **Agricultural Water Management**, Amsterdam, v. 146, p. 324–334, 2014.

STEDINGER, J.R.; VOGEL, R.M.; LEE, S.U.; BATCHELDER, R. Appraisal of the Generalized Likelihood Uncertainty Estimation (GLUE) method. **Water Resources Research**, Washington, v. 44, n. 12, W00B06, 2008.

ŠIMŮNEK, J.; HUANG, K.; VAN GENUCHTEN, M.T. **The HYDRUS code for simulating the one-dimensional movement of water, heat, and multiple solutes in variably-saturated media**. Riverside: U.S. Salinity Laboratory, 1998. 164 p. (Research Report, 144).

SUN, M.; ZHANG, X.; HUO, Z.; FENG, S.; HUANG, G.; MAO, X. Uncertainty and sensitivity assessments of an agricultural–hydrological model (RZWQM2) using the GLUE method. **Journal of Hydrology**, Amsterdam, v. 534, p. 19-30, 2016.

SUSHA, S.U.L.; SINGH, D.N.; BAGHINI, M.S. A critical review of soil moisture measurement. **Measurement**, Amsterdam, v. 54, p. 92-105, 2014.

VAN GENUCHTEN, M.T. A closed-form equation for predicting the hydraulic conductivity of unsaturated soils. **Soil Science Society of American Journal**, Madison, v. 44, n. 5, p. 892-898, 1980.

VAN GENUCHTEN, M.T.; NIELSEN, D.R. On describing and predicting the hydraulic properties of unsaturated soils. **Annales Geophysicae**, Gottingen, v. 3, n. 5, p. 615-628, 1985.

VAN DAM, J.C.; GROENENDIJK, P.; HENDRIKS, R.F.A.; KROES, J.G. Advances of modeling water flow in variably saturated soils with SWAP. **Vadose Zone Journal**, Madison, v. 7, n. 2, p. 640-653, 2008.

VERECKEN, H.; DIELS, J.; VAN ORSHOVEN, J.; FEYEN, J.; BOUMA, J. Functional evaluation of pedotransfer functions for the estimation of soil hydraulic properties. **Soil Science Society of American Journal**, Madison, v. 56, n. 5, p. 1371–1378, 1992.

VERECKEN, H.; WEYNANTS, M.; JAVAUX, M.; PACHEPSKY, Y.; SCHAAP, M.G.; VAN GENUCHTEN, M.T. Using pedotransfer functions to estimate the van Genuchten-Mualem soil hydraulic properties: a review. **Vadose Zone Journal**, Madison, v. 9, p. 820-975, 2010.

VERECKEN, H.; PACHEPSKY, Y.; SIMMER, C.; RIHANI, J.; KUNOTH, A.; KORRES, W.; GRAF, A.; FRANSSSEN, H.J.-H.; THIELE-EICH, I. On the role of patterns in understanding the functioning of soil–vegetation–atmosphere systems. **Journal of Hydrology**, Amsterdam, v. 542, p. 63–86, 2016.

VRUGT, J.A.; TER BRAAK, C.J.F.; CLARK, M.P.; HYMAN, J.M.; ROBINSON, B.A. Treatment of input uncertainty in hydrologic modeling: doing hydrology backward with Markov Chain Monte Carlo simulation. **Water Resources Research**, Washington, v. 44, n. 12, p. 5121–5127, 2008.

VRUGT, J.A.; TER BRAAK, C.J.F. DREAM(D): an adaptive Markov chain Monte Carlo simulation algorithm to solve discrete, noncontinuous, and combinatorial posterior parameter estimation problems. **Hydrological and Earth System Sciences**, Gottingen, v. 15, n. 12, p. 3701–3713, 2011.

WAGENER, T.; GUPTA, H.V. Model identification for hydrological forecasting under uncertainty. **Stochastic Environmental Research and Risk Assessment**, New York, v. 19, n. 6, p. 378-387, 2005.

WALKER, W.E.; HARREMOES, P.; ROTMANS, J.; VAN DER SLUIJS, J.P.; VAN ASSELT, M.B.A.; JANSSEN, P.; KRAYER VON KRAUSS, M.P. Defining uncertainty: A conceptual basis for uncertainty management in model-based decision support. **Integrated Assessment**, Vancouver, v. 4, n. 1, p. 5-17, 2003.

WORKMANN, S.R.; SKAGGS, R.W. Sensitivity of water management models to approaches for determining soil hydraulic properties, **Transaction of the ASAE**, Saint Joseph, v. 37, n. 1, p. 95–102, 1994.

#### 4 CONCLUDING REMARKS

Agro-hydrological models are powerful tools for predict and simulate water balance and crop yield providing reliable information for decision-making processes. However, although many agro-hydrological have been developed in the past decades, they implicitly are simplifications of natural systems, and include assumptions and generalizations in their structure and parameterization. Furthermore, uncertainties related to model input parameters, model structure and numerical solution are inherent to the modelling process.

The hydraulic properties characterization is still one the main issues in soil physics since soil water dynamics have a complex behavior, making its parameterization challenging. Many methodologies have been developed both for laboratory and field conditions, however they may provide diverging soil hydraulic properties for a given soil type. Moreover, related uncertainties are not readily provided by most of these methods. Added to these challenges, soil spatial variability either inherent or promoted by human activities, enhance the complexity of the characterization of the hydraulic properties.

One strategy to overcome these issues is to apply numerical methods to obtain the soil hydraulic properties. This methods enable to use data measured in the field from transient flow using parameter optimization algorithms. However, these methods require initial soil and boundary conditions, and are depended upon the optimization algorithms potential. The hydraulic properties uncertainties are readily available, which can be used both for assess the quality of the hydraulic properties calibration and further uncertainty analysis.

The modelling of natural systems deals with uncertainties. These uncertainties can be used to assess the reliability of model predictions and provide useful information for uncertainty reduction. However, the different sources of uncertainties and their inter dependence makes the uncertainty assessment complex. In agro-hydrological modelling, the parameters related to hydraulic properties have shown strong influence on the models predictions highlighting the importance of this study.

Despite the importance of identification and quantifications of these sources of uncertainties, efforts towards a systematic and integrated manner to assess the uncertainty analysis in agro hydrological modelling should be made. More studies involving numerical and stochastic methods should be performed to improve the understanding of natural systems.



**APPENDIX**



**Appendix A:** R algorithm used to perform the Latin Hypercube Sampling (LHS) and the stochastic realization of the SWAP model

```

# Realisation: Thalita Campos Oliveira and Jan G. Wesseling
# Date : May 28th 2018
-----

# Function to replace strings with values in template file
createInputFile <- function (pars, template, outputFile) {
  success = TRUE
  # pars should be a list
  if (!is.list(pars)){
    stop("Argument pars should be a list")
  }
  names(pars) <- paste("<", names(pars), ">", sep="")

  # Do parameters occur in template?
  n <- sapply(names(pars), function(x) (length(grep(x,template))))
  if (any(n == 0)){
    stop(paste(names(pars)[which(n == 0)], collapse = " "), " not
found in template!")
  }

  result <- template
  for (i in 1:length(pars)){
    result <- gsub(pattern = names(pars)[i], replacement =
pars[[i]], x=result)
  }

  # store result
  writeLines(text = result, con = outputFile)
  return(success)
}

#-----
# Inverse ecdf

```

```

inv_ecdf <- function(f) {
  x <- environment(f)$x
  y <- environment(f)$y
  approxfun(y,x, rule=2)
}
#-----
# main program
# read measured parameters for top layer
dataA <- read.csv("D:/LatinHypercube/Data/ParA.csv", sep="\t")
head(dataA)
# read measured parameters for subsoil
dataB <- read.csv("D:/LatinHypercube/Data/ParB.csv", sep="\t")
head(dataB)
# read correlation matrix
correlationMatrix <- read.csv("D:/LatinHypercube/Data/corr.csv",
sep=",", header = FALSE)
head(correlationMatrix)
#Create cumulative distribution functions and inverse
alfaA <- dataA$alfa
nA <- dataA$n
thetaRA <- dataA$tetar
thetaSA <- dataA$tetas
kSA <- dataA$ks
alfaB <- dataB$alfa
nB <- dataB$n
thetaRB <- dataB$tetar
thetaSB <- dataB$tetas
kSB <- dataB$ks
alfaA.ecdf <- ecdf(alfaA)
nA.ecdf <- ecdf(nA)
thetaRA.ecdf <- ecdf(thetaRA)
thetaSA.ecdf <- ecdf(thetaSA)

```

```
kSA.ecdf <- ecdf(kSA)
alfaB.ecdf <- ecdf(alfaB)
nB.ecdf <- ecdf(nB)
thetaRB.ecdf <- ecdf(thetaRB)
thetaSB.ecdf <- ecdf(thetaSB)
kSB.ecdf <- ecdf(kSB)
alfaA.ecdf.inverse <- inv_ecdf(alfaA.ecdf)
nA.ecdf.inverse <- inv_ecdf(nA.ecdf)
thetaRA.ecdf.inverse <- inv_ecdf(thetaRA.ecdf)
thetaSA.ecdf.inverse <- inv_ecdf(thetaSA.ecdf)
kSA.ecdf.inverse <- inv_ecdf(kSA.ecdf)
alfaB.ecdf.inverse <- inv_ecdf(alfaB.ecdf)
nB.ecdf.inverse <- inv_ecdf(nB.ecdf)
thetaRB.ecdf.inverse <- inv_ecdf(thetaRB.ecdf)
thetaSB.ecdf.inverse <- inv_ecdf(thetaSB.ecdf)
kSB.ecdf.inverse <- inv_ecdf(kSB.ecdf)
# Create parameter set
# number of draws
nRuns <- 250
# number of parameters
nParams <- 10
#rawParamSet <- randomLHS(nRuns, nParams)
# create parameter set
myLHS <- LHS(factors = c("alfaA", "nA", "thetaRA", "thetaSA", "kSA",
"alfaB", "nB", "thetaRB", "thetaSB", "kSB"), N = nRuns, method =
"random")
rawParamSet <- get.data(myLHS)
# Apply correlation
LHScorr <- LHScorr(rawParamSet, COR = correlationMatrix, method = "Pearson",
eps = 0.005, echo = TRUE, maxIt = 1000)
rawParamSet
# Create real parameters
```

```

realParams <- matrix(nrow = nrow(rowParamSet), ncol =
ncol(rowParamSet))

for (i in 1:nrow(realParams)){
  realParams[i,1] <- alfaA.ecdf.inverse(rowParamSet[i,1])
  realParams[i,2] <- nA.ecdf.inverse(rowParamSet[i,2])
  realParams[i,3] <- thetaRA.ecdf.inverse(rowParamSet[i,3])
  realParams[i,4] <- thetaSA.ecdf.inverse(rowParamSet[i,4])
  realParams[i,5] <- kSA.ecdf.inverse(rowParamSet[i,5])
  realParams[i,6] <- alfaB.ecdf.inverse(rowParamSet[i,6])
  realParams[i,7] <- nB.ecdf.inverse(rowParamSet[i,7])
  realParams[i,8] <- thetaRB.ecdf.inverse(rowParamSet[i,8])
  realParams[i,9] <- thetaSB.ecdf.inverse(rowParamSet[i,9])
  realParams[i,10] <- kSB.ecdf.inverse(rowParamSet[i,10])
}

realParams
# correct NA
for (i in 1:nrow(realParams)){
  for (j in 1:ncol(realParams)){
    k <- 0
    while ((is.na(realParams[i,j])) & (k < 100)){
      k <- k + 1
      rowParamSet[i,j] <- 1.01 * rowParamSet[i,j];
#      cat(k, rowParamSet[i,j], realParams[i,j])
      realParams[i,j] <- case_when(
        j==1 ~ alfaA.ecdf.inverse(rowParamSet[i,j]),
        j==2 ~ nA.ecdf.inverse(rowParamSet[i,j]),
        j==3 ~ thetaRA.ecdf.inverse(rowParamSet[i,j]),
        j==4 ~ thetaSA.ecdf.inverse(rowParamSet[i,j]),
        j==5 ~ kSA.ecdf.inverse(rowParamSet[i,j]),
        j==6 ~ alfaB.ecdf.inverse(rowParamSet[i,j]),
        j==7 ~ nB.ecdf.inverse(rowParamSet[i,j]),
        j==8 ~ thetaRB.ecdf.inverse(rowParamSet[i,j]),

```

```

        j==9 ~ thetaSB.ecdf.inverse(rawParamSet[i,j]),
        j==10 ~ kSB.ecdf.inverse(rawParamSet[i,j])
    )
}
}
}
realParams
# swap files
baseDir <- "d:\\LatinHypercube\\swaprun\\"
swpFileName <- paste(baseDir, "swap.swp", sep="")
wbaFileName <- paste(baseDir, "result.wba", sep="")
okFileName <- paste(baseDir, "swap.ok", sep="")
crzFileName <- paste(baseDir, "result.crz", sep="")
crpFileName <- paste(baseDir, "result.crp", sep="")
# read template file
swpTemplate <- "d:/LatinHypercube/Templates/Template.swp"
swpData <- readLines(con = swpTemplate)
# prepare dataframe for output
runs <- data.frame(Runoff = numeric(nRuns), qRootPos =
numeric(nRuns), qRootNeg = numeric(nRuns), evapSoil =
numeric(nRuns), qBot = numeric(nRuns))
runs$Runoff <- NA
runs$qRootPos <- NA
runs$qRootNeg <- NA
runs$evapSoil <- NA
runs$qBot <- NA
runs$yield <- NA
# make runs
for (i in 1:nrow(realParams)) {
    cat(paste("Processing ", i, " of ", nrow(realParams), "\n",
sep=""))
    # alfa-values > 0.1e-3

```

```

if(realParams[i,1] < 0.00011){
  alfaAc <- 0.00011
}
else
{
  alfaAc <- realParams[i,1]
}
if(realParams[i,6] < 0.00011){
  alfaBc <- 0.00011
}
else
{
  alfaBc <- realParams[i,6]
}
# put values into file
parameterValues <- list(
  alfaA = formatC(alfaAc, format = "f"),
  nA = formatC(realParams[i,2], format = "f"),
  thetaRA = formatC(realParams[i,3], format = "f"),
  thetaSA = formatC(realParams[i,4], format = "f"),
  kSA = formatC(realParams[i,5], format = "f"),
  alfaB = formatC(alfaBc, format = "f"),
  nB = formatC(realParams[i,7], format = "f"),
  thetaRB = formatC(realParams[i,8], format = "f"),
  thetaSB = formatC(realParams[i,9], format = "f"),
  kSB = formatC(realParams[i,10], format = "f")
)

success <- createInputFile(pars = parameterValues, template =
swpData, outputFile = swpFileName)

# run swap
runCommand <- paste(baseDir, "run.bat", sep="")
shell.exec(runCommand)

```

```

Sys.sleep(2)
while (!file.exists(okFileName)){
  Sys.sleep(1)
}
# read output if run is ok
if (file.exists(okFileName)){
  swapOutput <- read.csv(file = wbaFileName, header=TRUE, as.is =
TRUE, skip = 6)
  n = nrow(swapOutput)
  years <- 0
  runoff <- 0.0
  evap <- 0.0
  qBot <- 0.0
  for (k in 2:n){
    if (swapOutput$Day[k] == 1) {
      years <- years +1
      runoff <- runoff + swapOutput$RunOff[k-1]
      evap <- evap + swapOutput$Eact[k-1]
      qBot <- qBot + swapOutput$Bot[k-1]
    }
  }
  years <- years + 1
  runs$Runoff[i] <- 10.0 * (runoff + swapOutput$RunOff[n]) / years
  runs$evapSoil[i] <- 10.0 * (evap + swapOutput$Eact[n]) /years
  runs$qBot[i] <- 10.0 * (qBot + swapOutput$Bot[n]) / years
  crzOutput <- read.csv(file = crzFileName, header=TRUE, as.is =
TRUE, skip = 6)
  names(crzOutput) = c("Date", "Daynr", "Node", "Drz", "qRoot")
  myRootPos <- 0.0
  myRootNeg <- 0.0
  for (j in 1:nrow(crzOutput)){
    if (crzOutput$qRoot[j] > 0.0){

```

```

        myRootPos <- myRootPos + crzOutput$qRoot[j]
    }
else
{
    myRootNeg = myRootNeg + crzOutput$qRoot[j]
}
}
runs$qRootPos[i] <- 10.0 * myRootPos / years
runs$qRootNeg[i] <- 10.0 * myRootNeg / years
cropOutput <- read.csv(file = crpFileName, header = TRUE, as.is
= TRUE, skip=7)
oldSum <- 0.0
yield <- 0.0
years <- 0
for (j in 1:nrow(cropOutput)){
    newSum <- cropOutput$DWLVCROP[j] + cropOutput$DWLVSOIL[j] +
cropOutput$DWST[j] + cropOutput$DWRT[j] + cropOutput$DWSO[j]
    if ((newSum < 1.0) & (oldSum > 1.0)){
        yield <- yield + oldSum
        years <- years + 1
    }
    oldSum <- newSum
}
runs$yield[i] <- yield / years
}
else
{
    cat("Problem with Swap")
}
}

```